Results in Physics 65 (2024) 107995

Contents lists available at ScienceDirect

Results in Physics

journal homepage: www.elsevier.com/locate/rinp

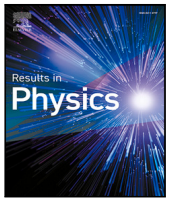

Modified Holling Tanner diffusive and non-diffusive predator–prey models: The impact of prey refuge and fear effect

Deepak Tripathi [a], Jai Prakash Tripathi [a], Satish Kumar Tiwari [b], Debaldev Jana [c], Li-Feng Hou [e], Yu Shi [d], Gui-Quan Sun [d,e,*], Vandana Tiwari [f], Joshua Kiddy K. Asamoah [g]

[a] Department of Mathematics, Central University of Rajasthan, Bandar Sindri, Kishangarh 305817, Ajmer, Rajasthan, India
[b] Assam Energy Institute, Sivasagar, a centre of Rajiv Gandhi Institute of Petroleum Technology, Sivasagar 785697, Assam, India
[c] Department of Mathematics, Ramakrishna Mission, Vivekananda Educational and Research Institute, Belur, India
[d] Department of Mathematics, North University of China, Taiyuan, Shanxi 030051, People's Republic of China
[e] Complex Systems Research Center, Shanxi University, Taiyuan, Shanxi 030006, People's Republic of China
[f] Gandhi Smarak PG College, Samodhpur, Jaunpur 223102, U.P., India
[g] Department of Mathematics, Kwame Nkrumah University of Science and Technology, Kuamsi, Ghana

ARTICLE INFO

Keywords:
Fear factor
Prey refuge
Self-diffusion
Beddington–DeAngelis type functional response
Hopf-bifurcation

ABSTRACT

The secondary consequences of predator species on prey species have substantial implications for population dynamics. A deeper comprehension of the dynamics between prey and predator can be achieved through the examination of indirect consequences. This work examines the dynamic behavior of a modified Holling-Tanner model. The interactions between the species are characterized by a functional response of the Beddington–DeAngelis type. Factors such as prey refuge, fear factor, disturbance intensity, and cross diffusion have been taken into account. The boundedness, feasibility of equilibrium points, their stability and restrictions for Hopf bifurcation of non-spatial model system are derived. The study explores the combined effects of prey refuge presence and fear factors on population dynamics. Furthermore, the investigation focuses on the stability of spatial self-diffusion and cross-diffusion model systems, as well as the specific conditions that lead to Turing instability. Ultimately, it has been shown that in the context of self-diffusion, a moderate level of fear promotes the survival of prey, whereas an excessive level of dread hinders the survival of prey. Concurrently, the mean density of prey exhibited a gradual decline as the refuge parameters increased. The spatial patterns of the population have also been investigated. As the mutual interference between prey populations intensifies, the spatial distribution of the prey population transitions from a clustered pattern to a combination of striped and clustered patterns, ultimately settling into a striped pattern. With the gradual growth of the half saturation constant, the prey population reached a state of uniform distribution. In the scenario of cross diffusion, when the prey is heavily impacted by the pursuit of predators, the fear effect, when appropriately used, did not have a significant impact on the survival of the prey. This work adds to the existing body of knowledge by revealing novel insights into the influence of indirect factors on the behavior of predator and prey populations.

Introduction

Gaining a comprehensive understanding of the dynamical behavior of prey and predators in mathematical biology is of utmost significance, particularly in ecosystems. This understanding is crucial for accurately anticipating the interactions between prey and predators and the levels of predation activity, which are essential for maintaining equilibrium and bio diversity [1]. Owing to rapid environmental change worldwide, habitat fragmentation, and the pressures of poaching, numerous species are on the brink of extinction [2]. Several extinct species include the *passenger pigeon*, the West African *black rhinoceros*, and the *Baiji white dolphin* [2]. Moreover, other species, like the *Amur leopard, gorillas*, and *sea turtles*, are currently facing the extinction challenges [3]. Preserving these species is essential for upholding ecological equilibrium and bio diversity. Relying solely on statistical data to forecast the impact of various characteristics on the intricate behavior of food webs may not always be sufficient. Thus, it is necessary to formulate these significant ecological concerns mathematically for better understanding.

The focus of numerous studies in recent decades have been solely on the direct consequences of predation for prey populations. Specifically, researchers have concentrated on predators' direct predation of prey

* Corresponding author.
E-mail address: gquansun@126.com (G.-Q. Sun).

https://doi.org/10.1016/j.rinp.2024.107995
Received 30 March 2024; Received in revised form 10 June 2024; Accepted 25 September 2024
Available online 28 September 2024

species. However, multiple data sources indicate that predator species' indirect influence on prey species significantly impacts species dynamics [4–7]. Nevertheless, the environment can only detect instances of direct killing. However, all prey within any given ecosystem respond to the risk of predation by exhibiting a range of anti-predator behaviors, including alterations in foraging patterns, the selection of new habitats, increased vigilance, and various psychological adaptations [8–14]. Typically, alarmed prey animals do not spend much time for searching food. However, when they are frightened by predators, they are compelled to adopt strategies like fasting, resulting in a reduction of the birth rate within that prey species and the lifespan of adult individuals [4,5]. As an illustration, birds respond to the auditory cues of a predator, and as a result of their fear response, they abandon their nesting site. The prey species, filled with fear, employs various tactics to minimize the chances of being hunted, including seeking out safe areas or times, gathering in groups, or reducing their movement to evade detection by predators. They identify alternative locations where they have a sense of safety. These anti-predator activities may benefit the survival of adult individuals. Still, the decision to move to a new place can occasionally have a detrimental impact on their reproductive success [4].

In 2011, Zanette et al. [15] conducted an experiment which demonstrated a 40% decrease in the reproductive success of song sparrows (*Melospiza melodia*) due to the threat posed by the presence of predator species. The decline in birth rate can be attributed to the anti-predator behavior, which negatively impacts both the birth rate and the survival of progeny. Hence, theoretical ecologists have observed that studying alone the immediate effects of species is inadequate; a comprehensive comprehension of species interactions necessitates the examination of indirect consequences as well. Indirect killing is a more powerful kind of predation compared to direct killing, as demonstrated in the studies [8,13,16,17].

Fear can have significant physiological effects on juvenile prey, perhaps leading to long-term harm in their adult life [15,18,19]. When prey animals perceive being hunted in a specific habitat, they may move to a different place with less danger of being attacked. Such changes could potentially lead to reduced overall fitness in the long run [4]. Predatory pressure-induced fear in prey population can lead to physiological stress, potentially manifesting in delayed sexual maturation, lengthened menstrual cycles with extended follicular phases, impeded ovulation, pregnancy loss (spontaneous abortion), and a prolonged postpartum period [4,18,20–24]. Wang et al. [25] integrated the fear effect into a prey-predator system. Several researchers [26–38] have recently examined the phenomenon of fear of predation in prey and demonstrated its significant impact on prey-predator dynamics. Furthermore, the researchers incorporated the fear response and the tendency of prey to seek sanctuary into their model [32,34].

Prey typically seek refuge in a secure area when they expect the possibility of being hunted. The refuge-seeking behavior displayed by prey impacts the coexistence dynamics between the prey and its predator [39]. Prey that conceals itself cannot be hunted, leading predators to seek alternative food sources and consume the prey that is accessible [40]. This might potentially lead to predators experiencing competition within their species [41–43]. The present work models both refuge-seeking behavior and anti-predatory conduct in prey. Assuming that the predator possesses a large radius of prey preferences, a prey-predator system is established by employing a modified version of the Holling-Tanner model [44–47]. The Beddington–DeAngelis functional response, as described in the Refs. [48,49], is utilized to depict the mutual interference between predators. The searching capability of the predator is adversely impacted by the intensity of prey refuge [39,45,50–57]. This validates the inclusion of prey refuge in terms of functional response. Recently, several researchers [58–65] have integrated refuge behavior into their prey-predator models.

The study [66] acknowledges the substantial impact that spatial and temporal elements have on ecological models. In a spatially extended system involving interacting species, the interaction between the predator and the prey is a crucial aspect, whereas the diffusion process becomes relevant when the predator tracks and avoids the prey species. Predator species possess the fundamental ability to capture prey, while prey species possess the inherent ability to escape predators. Typically, the speed at which the prey needs to flee is directly related to the speed at which the predator species moves around. Conversely, the attraction of predators to prey species leads them to approach each other. Thus the speed at which predators pursue their prey could directly be related to the speed at which the prey moves randomly. This phenomenon is commonly referred to as cross-diffusion. Notably, Kerner proposed the concept of cross-diffusion, as documented in his works from 1975 and 1959. Subsequently, Shigesada and colleagues included this concept into the competitive population system, as described in their publication from 1979. Diffusion is commonly regarded as a spatial transmission mechanism that moves from higher-density to lower-density areas. From a biological perspective, cross-diffusion theory elucidates how prey species employ a security mechanism to protect themselves from predator attacks.

The cross-diffusion coefficient could be negative, zero, or positive, whereas the self-diffusion coefficient is always positive. The positive cross-diffusion coefficient signifies that the population fluctuates in a manner where one species has a lower density, whereas the negative cross-diffusion coefficient indicates that a species moves diffusively when its density is higher. Comprehending the influence of geographical diffusion on the dynamics between prey and predators has posed a difficult challenge for bio-mathematicians and ecologists [67]. Climate variations, water currents, wind patterns, turbulence, and food supply changes, cause spatial displacement in both land and aquatic organisms. Hence, in a prey-predator scenario, the dynamics that occur in space and time hold great importance. Recently, numerous authors have examined the spatio-temporal dynamics of models in different fields [68–78]. The phenomenon of spatial diffusion in mathematical models incorporating refuge-seeking behavior [58,60,61,64] and anti-predatory behavior in prey [79–82] has extensively been investigated to date. This study incorporates the fear factor and prey refuge, which represent indirect predation, into a spatial prey-predator model. The main objectives of the present work are:

(*i*) to develop and analyze modified Holling Tanner spatial and non-spatial model systems in the presence of prey refuge, fear effects and mutual interference.

(*ii*) investigating the role of prey refuge in alterations of the interactions between prey and predator.

(*iii*) to examine the influence of fear effects on the stability and qualitative behaviors of spatial and non-spatial prey-predator interactions.

(*iv*) to provide ecological insights that how these factors (refuge, fear effects and mutual interference) affect the overall dynamics and long term outcomes of ecological systems.

The present investigation is organized as follows: The model has been described in Section "Mathematical model". Refer to Section "Analysis of non-Spatial model" for the mathematical analysis of a spatially-independent model including bifurcation analysis and impact of fear and refuge. Section "Stability of Spatial Model" covers the stability study of the spatial model system. Section "Turing instability of spatial system with cross diffusion" explores the Turing instability in spatial systems with cross-diffusion. Numerical simulations of non-spatial and spatial model systems are detailed in Section "Numerical results". The conclusion of this study has been discussed in Section "Conclusion".

Mathematical model

Assuming that the prey follow a logistic growth pattern in the absence of predation and fear effects. Their population dynamics can be divided into three components: the birth rate, the natural death

rate, and the density dependent death rate resulting from intra-specific competition. This leads to the following differential equation:

$$\frac{du}{dt} = au - du - bu^2, \tag{1}$$

where, u depicts the prey population, a is the birth rate of prey, d is the natural mortality rate of prey and b stands for the death rate due to intra-specific competition. Let v serves as the population of predator. Field experiments demonstrate that the fear effect reduces production. Consequently, we adjust Eq. (1) by multiplying the production term by a factor $f_1(l, v)$ which reflects the cost of anti predator defenses resulting from fear. Thus

$$\frac{du}{dt} = af_1(l, v)u - du - bu^2. \tag{2}$$

Here, the non-negative parameter l explains the level of fear which derives anti predator behaviors of the prey. Considering the ecological sense of l, v and $f_1(l, v)$, it is reasonable to assume that

$$f_1(0, v) = 1, f_1(l, 0) = 1, \lim_{l\to\infty} f_1(l, v) = 0, \lim_{v\to\infty} f_1(l, v) = 0, \frac{\partial f_1(l, v)}{\partial l} < 0, \frac{\partial f_1(l, v)}{\partial v} < 0.$$

While some arguments beliefs [83] suggest that fear could result in diminished adult survival rates due to physiological effects during youth, there is a lack of direct experimental evidence supporting this notion. Consequently, we do not include this factor as variable in our modeling efforts treating b and d as constant for the purpose of this study.

Further, we introduce a predation term $g(u, v)$ to Eq. (2) resulting in the following differential equation related to rate of growth of prey species:

$$\frac{du}{dt} = af_1(l, v)u - du - bu^2 - g(u, v). \tag{3}$$

There are some famous functional responses in the predator–prey interaction system, namely, Holling, Beddington–DeAngelis, Monod–Haldane, Michaelis–Menten, ratio-dependent, Leslie–Gower and Crowley–Martin type. Here the Beddington–DeAngelis type interaction between the predator and prey species has been assumed. If m symbolizes the sanctuary safeguarding prey, then $(1 - m)u$ denotes the prey exclusively accessible to predators. Thus the predation term takes the following form:

$$g(u, v) = \frac{p(1 - m)uv}{cv + b_1(1 - m)u + a_1},$$

where, the parameter p signifies the predation rate, whereas m (where $0 \le m < 1$) denotes the amount of refuge accessible to the prey. The parameter c measures the extent of interference among predators. The parameters b_1 and a_1 indicate the mutual interference between prey and the half-saturation constant, respectively.

Now, we incorporate a particular type of expression for $f_1(l, v)$ that satisfy the above mentioned property. Therefore, the Eq. (3) has the following form

$$\frac{du}{dt} = \frac{au}{1 + lv} - du - bu^2 - \frac{p(1 - m)uv}{cv + b_1(1 - m)u + a_1}. \tag{4}$$

The predator–prey system of the Leslie type was first introduced by Leslie [84]. The Leslie–Gower term has the following form for predator species in the presence of prey refuge

$$\frac{dv}{dt} = \delta v - \frac{\beta v^2}{(1 - m)u + b_2}, \tag{5}$$

where, the symbol δ signifies the growth rate of predator species, while β is the conversion coefficient of prey-provided food into predator birth. The positive constant b_2 denotes the half saturation constant.

Han et al. [80] examined the consequences of cross-diffusion in a predator–prey model incorporating the fear effect, considering the prey's group defense and the predator's random movement towards areas with lower prey density. So it becomes crucial to investigate the proportion of prey involved during the interactions of prey-predator and the percentage of prey seeking refuge for safety. The dynamics of the model could significantly be influenced by the presence of prey. Thus, this study examines a two-species reaction–diffusion model including the impact of fear and prey refuge incorporating the Beddington–DeAngelis type functional response. Since spatial prey–predator models are essential for capturing the complexity of ecological interactions in real-world landscapes, leading to better understanding, prediction, and management of ecological systems. Therefore, the dynamics of interacted prey and predator species is described by the following set of partial differential equations:

$$\frac{\partial u}{\partial t} = \frac{au}{1 + lv} - du - bu^2 - \frac{p(1 - m)uv}{cv + b_1(1 - m)u + a_1} + D_1\nabla^2 u, \tag{6}$$

$$\frac{\partial v}{\partial t} = \delta v - \frac{\beta v^2}{(1 - m)u + b_2} + D_2\nabla^2 v, \tag{7}$$

along with initial restrictions

$$u(x, y, 0) > 0, \quad v(x, y, 0) > 0, \quad \text{for } (x, y) \in \Omega, \tag{8}$$

and boundary restrictions

$$\frac{\partial u}{\partial n} = \frac{\partial v}{\partial n} = 0, \ (x, y) \in \partial\Omega \ \text{ for all } t. \tag{9}$$

The Laplacian operator ∇^2 is frequently utilized for space of two-dimension. The diffusion coefficients D_1 and D_2 indicate the rates at which the prey and predator diffuse, respectively. The vector n denotes the outward normal direction of the border $\partial\Omega$.

The biological meaning of all the non-negative parameters in the model system (6)–(7) with their precise units have been summarized in the Table 1.

Analysis of non-spatial model

Initially, we concentrate on examining the well-posedness of the non-spatial model. We also analyze the stability of all possible equilibria that occur in the non-spatial model. The model system without diffusion (associated with the spatial system (6)–(7)) is given by the following system of ordinary differential equations:

$$\frac{du}{dt} = \frac{au}{1 + lv} - du - bu^2 - \frac{p(1 - m)uv}{cv + b_1(1 - m)u + a_1} = uf_2(u, v), \tag{10}$$

$$\frac{dv}{dt} = \delta v - \frac{\beta v^2}{(1 - m)u + b_2} = vf_3(u, v). \tag{11}$$

The initial conditions are given by: $u(0) > 0$, $v(0) > 0$.

Well-posedness

In the following lemma, we have demonstrated that any solution of the model (10)–(11) is both bounded and eventually contained within the set Λ.

Lemma 1. *The set*

$$\Lambda = \left\{(u(t), v(t)) : 0 \le u(t) \le \frac{a}{b}, \ 0 \le v(t) \le \frac{\delta\{a(1 - m) + bb_2\}}{b\beta}\right\},$$

forms a positively invariant set and attracts all solutions that begin within the positive quadrant's interior.

Proof. From Eq. (10) with initial restriction, we have

$$u(t) = u(0)exp\left(\int_0^t \left[\frac{a}{1 + lv} - d - bu - \frac{p(1 - m)v}{cv + b_1(1 - m)u + a_1}\right]dT\right) > 0. \tag{12}$$

From Eq. (11) with initial condition, we get

$$v(t) = v(0)exp\left(\int_0^t \left[\delta - \frac{\beta v}{(1 - m)u + b_2}\right]dT\right) > 0. \tag{13}$$

Table 1
Biological explanations of the parameters associated with the model (6)–(7).

Parameters	Biological meaning	Unit
a	Prey species' growth rate	$[\text{time}]^{-1}$
l	Fear factor	$[\text{density}]^{-1}$
d	Mortality rate of prey species due to natural causes	$[\text{time}]^{-1}$
b	Mortality rate of prey species caused by competition within the same species	$[\text{density}]^{-1}[\text{time}]^{-1}$
p	Predation rate	$[\text{time}]^{-1}$
m	Prey refuge $(0 \le m < 1)$	–
c	Mutual interference between predators	–
b_1	Mutual interference between prey species	–
a_1	Half saturation constant	[density]
δ	Growth rate of the predator species	$[\text{time}]^{-1}$
β	The amount of food provided by prey is turned into predator offspring.	–
b_2	Half saturation constant for predator	[density]
D_1	Rate coefficient for the diffusion of prey species itself	$[\text{length}]^2[\text{time}]^{-1}$
D_2	Rate coefficient of self-diffusion for predators	$[\text{length}]^2[\text{time}]^{-1}$

Thus, based on Eqs. (12) and (13), every solutions of the model (10)–(11) are included within $\mathbb{R}^2_+ = \{(u,v) : u > 0, v > 0\}$ for the specified initial circumstances. From the first equation of the non-spatial model (10)–(11), we derive

$$\frac{du}{dt} \le u(a - bu).$$

Using the comparison principle, we have

$$\lim_{t\to\infty} \sup u(t) \le \frac{a}{b}. \tag{14}$$

Also, using the second equation of model (10)–(11) and inequality (14), we get

$$\frac{dv}{dt} \le v\left(\delta - \frac{b\beta v}{(1-m)a + bb_2}\right).$$

In the same way, we have

$$\lim_{t\to\infty} \sup v(t) \le \frac{\delta\{a(1-m) + bb_2\}}{b\beta}. \tag{15}$$

Thus, from inequality (14) and (15) along with positivity of solutions, we summarize that every solutions of non-spatial system are bounded in $\mathbb{R}^2_+$. □

Stability analysis

Regarding the equilibrium points, we equate $\frac{du}{dt} = 0, \frac{dv}{dt} = 0$. Model (10)–(11) has four types of ecologically feasible equilibrium points:

(i) $E_0(0,0)$ is a species free equilibrium point;
(ii) $E_1(\tilde{u},0)$; where $\tilde{u} = \frac{(a-d)}{b}$ is feasible if and only if $a > d$, i.e., predator free state occurs only when the growth rate of prey species is greater than its natural death rate;
(iii) the equilibrium point free from prey is $E_2(0,\tilde{v})$, where $\tilde{v} = \frac{b_2\delta}{\beta}$;
(iv) the coexisting equilibrium points are $E_3\left(u^*, \frac{(1-m)\delta u^* + b_2\delta}{\beta}\right)$, where u^* are the positive solutions of following cubic equation, $A_1u^3 + B_1u^2 + C_1u + L_1 = 0$, where,

$$A_1 = \delta bl(1-m)^2(b_1\beta + c\delta) > 0,$$

$$B_1 = (1-m)(l\delta(1-m)(b_1d\beta + (cd + p(1-m))\delta) + b(b_1\beta(\beta + b_2l\delta) + \delta(c\beta + a_1l\beta + 2b_2cl\delta))) > 0,$$

$$C_1 = (a_1b + b_1(a-d)(m-1))\beta^2 + (bb_2(c + a_1l) + ac(m-1) - (m-1)(d(c + a_1l + b_1b_2l) + p(1-m)))\beta\delta + b_2l(bb_2c - 2(m-1)(cd + p(1-m)))\delta^2,$$

$$L_1 = -a\beta(a_1\beta + b_2c\delta) + (\beta + b_2l\delta)(a_1d\beta + b_2(cd + p(1-m))\delta).$$

Obviously, the number of coexisting equilibria directly depend on the sign of C_1 and L_1. Thus, it could be summarized as follows:

(a) If $C_1 > 0$ and $L_1 > 0$ then no coexisting equilibrium point comes in picture;
(b) if $L_1 < 0$ then there is feasibility of one coexisting equilibrium point;
(c) if $C_1 < 0$ and $L_1 > 0$ then two coexisting equilibria are admissible.
Thus, the model system (10)–(11) has at most two coexisting equilibria.

Theorem 2. *For species free equilibrium point $E_0(0,0)$, we have*

(i) if $a > d$, then E_0 exist in unstable mode;
(ii) if $a < d$, then E_0 is a saddle point along with stable manifold in u-direction and unstable manifold in v-direction.

Proof. The eigenvalues of Jacobian matrix at E_0 are $\nu_1 = (a-d)$ and $\nu_2 = \delta$. Thus, if $a > d$ then $\nu_1 > 0$ and $\nu_2 > 0$, hence $E_0(0,0)$ is unstable. If $a < d$ then $\nu_1 < 0$ and $\nu_2 > 0$, therefore E_0 is a saddle point. □

For predator free equilibrium point $E_1\left(\frac{a-d}{b}, 0\right)$, the eigenvalues associated with Jacobian matrix are $\nu_1 = (d-a)$ and $\nu_2 = \delta$. By the feasibility condition of E_1, it is obvious that $\nu_1 < 0$ and $\nu_2 > 0$. Therefore, the theorem presented below is

Theorem 3. *The equilibrium point free from predator E_1 is a saddle point with stable manifold in u-direction and unstable manifold in v-direction.*

For prey free equilibrium point $E_2\left(0, \frac{b_2\delta}{\beta}\right)$, the eigenvalues corresponding to Jacobian matrix are $\nu_1 = \frac{a\beta}{\beta + lb_2\delta} - d - \frac{p(1-m)b_2\delta}{cb_2\delta + a_1\beta}$ and $\nu_2 = -\delta$, thus we have

Theorem 4.

(i) The equilibrium point free from prey E_2 is locally asymptotically stable if $\frac{a\beta}{\beta + lb_2\delta} < d + \frac{p(1-m)b_2\delta}{cb_2\delta + a_1\beta}$, i.e., the birth and death rate of prey species play a vital role to maintain the stability of E_2,
(ii) if $\frac{a\beta}{\beta + lb_2\delta} > d + \frac{p(1-m)b_2\delta}{cb_2\delta + a_1\beta}$, then E_2 is saddle point with unstable manifold in u-direction and stable manifold in v-direction.

The Jacobian matrix evaluated at $E_i(u^*, v^*)$ (i=3, 4) is given by

$$J = \begin{pmatrix} u^*\left(-b + \frac{b_1 p(1-m)^2 v^*}{\left(cv^* + b_1(1-m)u^* + a_1\right)^2}\right) & u^*\left(-\frac{al}{(1+lv^*)^2} - \frac{p(1-m)\left(b_1(1-m)u^* + a_1\right)}{\left(cv^* + b_1(1-m)u^* + a_1\right)^2}\right) \\ \frac{\beta(1-m)v^{*2}}{\left((1-m)u^* + b_2\right)^2} & -\frac{\beta v^*}{(1-m)u^* + b_2} \end{pmatrix}$$

$$= \begin{pmatrix} u^*\left(-b + \frac{b_1 p(1-m)^2 v^*}{\left(cv^* + b_1(1-m)u^* + a_1\right)^2}\right) & u^*\left(-\frac{al}{(1+lv^*)^2} - \frac{p(1-m)\left(b_1(1-m)u^* + a_1\right)}{\left(cv^* + b_1(1-m)u^* + a_1\right)^2}\right) \\ \frac{(1-m)\delta^2}{\beta} & -\delta \end{pmatrix}$$

$$= \begin{pmatrix} j_{11} & j_{12} \\ j_{21} & j_{22} \end{pmatrix}.$$

Now, we can determine the eigenvalues of the aforementioned matrix by solving the following characteristic equation

$$\nu^2 - \mathrm{tr}(J)\nu + \det(J) = 0, \tag{16}$$

where, $tr(J) = \frac{pb_1(1-m)^2u^*v^*}{(a_1+b_1(1-m)u^*+cv^*)^2} - (bu^* + \delta)$,
$det(J) = \frac{1}{(a_1+b_1(1-m)u^*+cv^*)^2(1+lv^*)^2\beta} u^*\delta\{2a_1b(b_1(1-m)u^* + cv^*)(1+lv^*)^2\beta + b(b_1(1-m)u^* + cv^*)^2(1+lv^*)^2\beta + a_1(1-m)(2alb_1(1-m)u^* + 2alcv^* + (1-m)p(1+lv^*)^2)\delta + a_1^2(b(1+lv^*)^2\beta + al(1-m)\delta) + (1-m)(alb_1^2(1-m)^2u^{*2}\delta + alc^2v^{*2}\delta - b_1(1-m)(-2alcu^*v^*\delta + p(1+lv^*)^2(v^*\beta - (1-m)u^*\delta)))\} > 0.$

Theorem 5. *The equilibrium point E_i (i=3, 4) is locally asymptotically stable if $b_1p(1-m)^2u^*v^* < (bu^* + \delta)(a_1 + b_1(1-m)u^* + cv^*)^2$.*

Proof. Due to the well-established nature of the underlying concepts, a formal proof is not provided. □

Theorem 6. *Suppose the following inequality hold in Λ*

$$b > \frac{pb_1(1-m)^2v^*}{A_3(u,v)}, \tag{17}$$

$$\left(\frac{al}{A_2(v)} + \frac{pb_1(1-m)^2u^* - a_1p(1-m)}{A_3(u,v)} - \frac{\alpha_1 v^*}{A_4(u)}\right)^2 < 4\left(b - \frac{pb_1(1-m)^2v^*}{A_3(u,v)}\right)\left(\frac{\alpha_1(1-m)\beta u^* + \alpha_1 b_2\beta}{A_4(u)}\right), \tag{18}$$

then the equilibrium point $E_i(u^*, v^*)$ exhibits global asymptotic stability for all solutions originating within the interior of the positive quadrant Λ, where $A_i(i = 2, 3, 4)$ is mentioned in the proof part.

Proof. For equilibrium points of the model system (10)–(11), we have

$$d = \frac{a}{1+lv^*} - bu^* - \frac{p(1-m)v^*}{cv^* + b_1(1-m)u^* + a_1} \text{ and } \delta = \frac{\beta v^*}{(1-m)u^* + b_2}.$$

So from above Eqns. of equilibrium points, model (10)–(11) reduces in the following form:

$$\frac{du}{dt} = u\left(\left(\frac{a}{1+lv} - \frac{a}{1+lv^*}\right) - \left(\frac{p(1-m)v}{cv + b_1(1-m)u + a_1} - \frac{p(1-m)v^*}{cv^* + b_1(1-m)u^* + a_1}\right) - b(u-u^*)\right),$$

$$\frac{dv}{dt} = v\left(\frac{-\beta v}{(1-m)u + b_2} + \frac{\beta v^*}{(1-m)u^* + b_2}\right).$$

Now, we define $P(u, v) : \mathbb{R}^2 \to \mathbb{R}$ in such a way that

$$P(u, v) = P_1(u, v) + P_2(u, v),$$

where $P_1(u, v) = u - u^* - u^* ln\left(\frac{u}{u^*}\right)$ and $P_2(u, v) = \alpha_1\left(v - v^* - v^* ln\left(\frac{v}{v^*}\right)\right)$. Here, α_1 is a positive constant and defined as below.

Clearly, this function $P(u, v)$ is well defined and continuous on $Int(\mathbb{R}^2)$ except $E_i(u^*, v^*)$ and vanishes at $E_i(u^*, v^*)$. Further, $\frac{\partial P_1(u,v)}{\partial u} > 0$ when $u > u^*$, $\frac{\partial P_1(u,v)}{\partial u} < 0$ when $u < u^*$ and $\frac{\partial P_2(u,v)}{\partial v} > 0$ when $v > v^*$ and $\frac{\partial P_2(u,v)}{\partial v} < 0$ when $u < u^*$. Thus, $P(u, v)$ attains minimum value at (u^*, v^*). Now

$$\frac{dP_1}{dt} = \frac{(u-u^*)}{u}\frac{du}{dt} = (u-u^*)\left(\left(\frac{a}{1+lv} - \frac{a}{1+lv^*}\right) - b(u-u^*) - \left(\frac{p(1-m)v}{cv + b_1(1-m)u + a_1} - \frac{p(1-m)v^*}{cv^* + b_1(1-m)u^* + a_1}\right)\right),$$

$$\frac{dP_2}{dt} = \alpha_1\frac{(v-v^*)}{v}\frac{dv}{dt} = \alpha_1(v-v^*)\left(\frac{-\beta v}{(1-m)u + b_2} + \frac{\beta v^*}{(1-m)u^* + b_2}\right).$$

Thus, after some simplification the derivative of $P(u, v)$ is given by

$$\frac{dP}{dt} = \left(\frac{pb_1(1-m)^2v^*}{A_3(u,v)} - b\right)(u-u^*)^2 - \left(\frac{al}{A_2(v)} + \frac{pb_1(1-m)^2u^*}{A_3(u,v)} - \frac{a_1p(1-m)}{A_3(u,v)} - \frac{\alpha_1 v^*}{A_4(u)}\right) \times (u-u^*)(v-v^*) - \left(\frac{\alpha_1(1-m)\beta u^* + \alpha_1 b_2\beta}{A_4(u)}\right)(v-v^*)^2 \tag{19}$$

where, $A_2(v) = (1+lv)(1+lv^*)$, $A_3(u, v) = (cv + b_1(1-m)u + a_1)(cv^* + b_1(1-m)u^* + a_1)$ and $A_4(u) = \left((1-m)u + b_2\right)\left((1-m)u^* + b_2\right)$.

The Eq. (19) could be reduced in the following form

$$\frac{dP}{dt} = -m_{11}(u-u^*)^2 + m_{12}(u-u^*)(v-v^*) - m_{22}(v-v^*)^2, \tag{20}$$

where, $m_{11} = \left(b - \frac{pb_1(1-m)^2v^*}{A_3(u,v)}\right)$, $m_{12} = -\left(\frac{al}{A_2(v)} + \frac{pb_1(1-m)^2u^*}{A_3(u,v)} - \frac{a_1p(1-m)}{A_3(u,v)} - \frac{\alpha_1 v^*}{A_4(u)}\right)$ and $m_{22} = \frac{\alpha_1(1-m)\beta u^* + \alpha_1 b_2\beta}{A_4(u)}$.

For $\frac{dP}{dt}$ to be negative definite, the following inequalities must be satisfied:

$$m_{11} > 0, m_{22} > 0 \text{ and } m_{12}^2 < 4m_{11}m_{22}.$$

Hence the theorem follows. □

Transcritical bifurcation

Firstly, let us define, $f(u, v) = \frac{au}{1+lv} - du - bu^2 - \frac{p(1-m)uv}{cv + b_1(1-m)u + a_1}$ and $g(u, v) = \delta v - \frac{\beta v^2}{(1-m)u + b_2}$. The Jacobian matrix evaluated at trivial equilibrium point $E_0(0, 0)$ is

$$J_{E_0} = \begin{bmatrix} (a-d) & 0 \\ 0 & \delta \end{bmatrix},$$

J_{E_0} possess zero eigenvalue if $a = d$. Now let us consider that X and Y be the eigenvectors of J_{E_0} and $J_{E_0}^T$ corresponding to zero eigenvalue, respectively. Thus we obtain

$$X = \begin{pmatrix} x_1 \\ x_2 \end{pmatrix} = \begin{pmatrix} 1 \\ 0 \end{pmatrix}, \quad Y = \begin{pmatrix} y_1 \\ y_2 \end{pmatrix} = \begin{pmatrix} 1 \\ 0 \end{pmatrix}.$$

Further, we compute the expression Δ_1, Δ_2 and Δ_3 for ensuring the transcritical bifurcation as discussed in Sotomayor's Theorem [85]. So we have

$$\Delta_1 = Y^T[F_a(0,0)] = \begin{bmatrix} 1 & 0 \end{bmatrix}\begin{bmatrix} 0 \\ 0 \end{bmatrix} = 0,$$

$$\Delta_2 = Y^T[DF_a(0,0)] = \begin{bmatrix} 1 & 0 \end{bmatrix}\begin{bmatrix} 1 \\ 0 \end{bmatrix} = 1 \neq 0,$$

$\Delta_3 = Y^T[D^2F[(0,0),a](X,X)] = y_1(f_{uu}x_1^2 + 2f_{uv}x_1x_2 + f_{vv}x_2^2) + y_2(g_{uu}x_1^2 + 2g_{uv}x_1x_2 + g_{vv}x_2^2) = -2b \neq 0$. Hence by Sotomayor's theorem, E_0 experiences a transcritical bifurcation if $a = d$.

Theorem 7. *The model (10)–(11) undergoes a transcritical bifurcation around the trivial equilibrium point $E_0(0,0)$ with respect to bifurcation parameter a, if $a = a^{TC} = d$, where a^{TC} is the critical value of bifurcation parameter.*

Hopf bifurcation

Let us assume that β is equal to the product of ξ and δ, where ξ is greater than zero. The Jacobian matrix for the positive interior equilibrium $E_3(u^*, v^*)$ is:

$$J(E_3) = \begin{pmatrix} u^*\left(-b + \frac{pb_1(1-m)^2v^*}{(cv^*+b_1(1-m)u^*+a_1)^2}\right) & u^*\left(-\frac{al}{(1+lv^*)^2} - \frac{p(1-m)(b_1(1-m)u^*+a_1)}{(cv^*+b_1(1-m)u^*+a_1)^2}\right) \\ \frac{(1-m)\delta}{\xi} & -\delta \end{pmatrix}.$$

The matrix's trace and determinant are given by

$$\mathrm{tr}(J(E_3)) = u^*\left(-b + \frac{pb_1(1-m)^2v^*}{(cv^* + b_1(1-m)u^* + a_1)^2}\right) - \delta,$$

$$\det(J(E_3)) = -\delta u^*\left(-b + \frac{pb_1(1-m)^2v^*}{(cv^*+b_1(1-m)u^*+a_1)^2}\right) + \frac{(1-m)\delta}{\xi}u^*\left(\frac{al}{(1+lv^*)^2} + \frac{p(1-m)(b_1(1-m)u^*+a_1)}{(cv^*+b_1(1-m)u^*+a_1)^2}\right).$$

Suppose $\det(J(E_3)) > 0$ and determine $\delta_{cr} = u^*\left(-b + \frac{pb_1(1-m)^2v^*}{(cv^*+b_1(1-m)u^*+a_1)^2}\right)$. As $\det(J(E_3)) > 0$, thus the stability of E_3 is established by $\mathrm{tr}(J(E_3))$. When $\delta > \delta_{cr}$, the equilibrium point E_3 is locally asymptotically stable. When $\delta < \delta_{cr}$, the equilibrium point E_3 exist in unstable mode. When $\delta = \delta_{cr}$, $\mathrm{tr}(J(E_3)) = 0$. Since $\det(J(E_3)) > 0$, therefore the Jacobian matrix $J(E_3)$ has only a pair of simple purely imaginary eigenvalue. The characteristic equation corresponding to matrix $J(E_3)$ is

$$\nu^2 - \mathrm{tr}(J(E_3))\nu + \det(J(E_3)) = 0. \tag{21}$$

Substituting $\nu = \eta + i\phi$ in Eq. (21) near $\delta = \delta_{cr}$, and analyzing real and imaginary part we get

$$\eta^2 - \phi^2 - \eta\mathrm{tr}(J(E_3)) + \det(J(E_3)) = 0, \tag{22}$$

$$2\eta\phi - \phi\mathrm{tr}(J(E_3)) = 0. \tag{23}$$

From Eq. (23), we have

$$\eta = \frac{1}{2}\mathrm{tr}(J(E_3)). \tag{24}$$

Eq. (24) rewritten as

$$\mathrm{Re}(\nu(\delta)) = \frac{1}{2}\mathrm{tr}(J(E_3)). \tag{25}$$

Taking derivative of Eq. (25) with respect to δ, we obtain

$$\frac{d(\mathrm{Re}(\nu(\delta)))}{d\delta} = -\frac{1}{2} \neq 0. \tag{26}$$

Therefore the transversality condition holds. Following theorem summarizes the above discussion.

Theorem 8. *Let $\det(J(E_3)) > 0$ and the critical value of δ is given as*

$$\delta_{cr} = u^*\left(-b + \frac{pb_1(1-m)^2v^*}{(cv^* + b_1(1-m)u^* + a_1)^2}\right),$$

then model (10)–(11) experiences Hopf bifurcation around E_3 at $\delta = \delta_{cr}$.

Stability of limit cycle

We compute the Lyapunov coefficient σ at the equilibrium point E_3 of the system in order to assess the stability of the limit cycle. For the same, we shift the function $E_3(u^*, v^*)$ of the system (10)–(11) to the origin using the transformation $u = \hat{u} - u^*$ and $v = \hat{v} - v^*$. The system (10)–(11) near the origin can be expressed as

$$\frac{d\hat{u}}{dt} = \alpha_{10}\hat{u} + \alpha_{01}\hat{v} + \alpha_{20}\hat{u}^2 + \alpha_{11}\hat{u}\hat{v} + \alpha_{02}\hat{v}^2 + \alpha_{30}\hat{u}^3 + \alpha_{21}\hat{u}^2\hat{v} + \alpha_{12}\hat{u}\hat{v}^2 + \alpha_{03}\hat{v}^3 + F_1(\hat{u},\hat{v}),$$

$$\frac{d\hat{v}}{dt} = \beta_{10}\hat{u} + \beta_{01}\hat{v} + \beta_{20}\hat{u}^2 + \beta_{11}\hat{u}\hat{v} + \beta_{02}\hat{v}^2 + \beta_{30}\hat{u}^3 + \beta_{21}\hat{u}^2\hat{v} + \beta_{12}\hat{u}\hat{v}^2 + \beta_{03}\hat{v}^3 + F_2(\hat{u},\hat{v}),$$

where, $F(u,v) = uf_2(u,v)$, $G(u,v) = vf_3(u,v)$, $\alpha_{ij} = \frac{1}{(i+j)!}\frac{\partial^{i+j}F}{\partial x^i\partial y^j}|_{(u^*,v^*)}$, $\beta_{ij} = \frac{1}{(i+j)!}\frac{\partial^{i+j}G}{\partial x^i\partial y^j}|_{(u^*,v^*)}$ and $F_i(\hat{u},\hat{v})$ $(i = 1, 2)$ are power series in powers of $\hat{u}^i\hat{v}^j$ satisfying $i + j \geq 4$.

Referring to the Lyapunov coefficient (σ) in a general planar system (10)–(11) (as mentioned in [85]) is given by: $\sigma = -\frac{3\pi}{2\alpha_{01}\Delta^{\frac{3}{2}}}\{[\alpha_{10}\beta_{10}(\alpha_{11}^2 + \alpha_{11}\beta_{02} + \alpha_{02}\beta_{11}) + \alpha_{10}\alpha_{01}(\beta_{11}^2 + \alpha_{20}\beta_{11} + \alpha_{11}\beta_{02}) + \beta_{10}^2(\alpha_{11}\alpha_{02} + 2\alpha_{02}\beta_{02}) - 2\alpha_{10}\beta_{10}(\beta_{02}^2 - \alpha_{02}\alpha_{20}) - 2\alpha_{10}\alpha_{01}(\alpha_{20}^2 - \beta_{20}\beta_{02}) - \alpha_{01}^2(2\alpha_{20}\beta_{20} + \beta_{11}\beta_{20}) + (\alpha_{01}\beta_{10} - 2\alpha_{10}^2)(\beta_{11}\beta_{02}^2 - \alpha_{11}\alpha_{20})] - (\alpha_{10}^2 + \alpha_{01}\beta_{10})[3(\beta_{10}\beta_{03} - \alpha_{01}\alpha_{30}) + 2\alpha_{10}(\alpha_{21} + \beta_{12}) + (\beta_{10}\alpha_{12} - \alpha_{01}\beta_{21})]\}$, where, $\Delta = \alpha_{10}\beta_{01} - \alpha_{01}\beta_{10}$.

The Lyapunov coefficient (σ) results from the algebraic combination of α_{ij} and β_{ij}. The sign of σ cannot be predicted due to complex algebraic expression. Hence, we present the following numerical example:

Numerical example

Consider $a = 0.6$, $d = 0.3$, $p = 0.15$, $b = 0.1$, $b_1 = 6$, $a_1 = 0.01$, $c = 0.5$, $\beta = 0.016$, $b_2 = 0.015$, $m = 0.01$, $l = 4$. For these parametric values, the Hopf bifurcation occurs at threshold value $\delta = \delta_{cr} = 0.03$. The value of σ for these parametric values is -1606.69 which is less than 0. Thus, the Hopf bifurcation is of supercritical type. Hence, a stable limit cycle is created around $E_3(u^*, v^*) = (0.0786, 0.1741)$. A limit cycle is evident in Fig. 4(d).

Consequences of fear factor (l) and prey refuge (m) on species density

Impact of fear factor (l) on prey and predator density

Since the prey density for the coexisting equilibria is evaluated through positive solution of the equation $A_1u^3 + B_1u^2 + C_1u + L_1 = 0$. We aim to analyze the impact of varying fear factors on prey population levels. Thus, we differentiate the above mentioned equation with respect to l

$$\left.\frac{du}{dl}\right|_{u=u^*} = -\left.\frac{(u^3\frac{dA_1}{dl} + u^2\frac{dB_1}{dl} + u\frac{dC_1}{dl} + \frac{dL_1}{dl})}{(3A_1u^2 + 2B_1u + C_1)}\right|_{u=u^*},$$

where, $\frac{dA_1}{dl} = b\delta(1-m)^2(b_1\beta + c\delta) > 0$, $\frac{dB_1}{dl} = (1-m)(b\delta(a_1\beta + b_1b_2\beta + 2b_2c\delta) + (1-m)\delta(b_1\beta d + (cd + p - mp)\delta)) > 0$, $\frac{dC_1}{dl} = (a_1bb_2 + d(a_1 + b_1b_2)(1-m))\beta\delta + b_2(bb_2c + 2(1-m)(cd + p - mp))\delta^2 > 0$, $\frac{dL_1}{dl} = b_2\delta(a_1d\beta + b_2(cd + p - mp)\delta) > 0$. A_1, B_1, C_1 and L_1 have same meaning as mentioned in Section "Stability analysis". If the coexisting equilibria exist and $l > \frac{P_3}{Q_3}$ hold, i.e., the fear factor (l) is greater than a threshold value then the prey density starts to decrease, where, $P_3 = \beta(a(1-m)(b_1\beta + c\delta) - a_1b\beta - bb_2c\delta - (1-m)(b_1d\beta + (cd + p(1-m))\delta))$, $Q_3 = \delta(a_1(bb_2 + d(1-m))\beta + b_2(bb_2c\delta + (1-m)(b_1d\beta + 2(cd + p(1-m))\delta)))$. This indicates that the fear factor leaves negative impact on prey density when fear factor crosses a level.

The predator density for coexisting equilibria is calculated as follows: $v = \frac{(1-m)\delta u + b_2\delta}{\beta}$. The derivative of v with regard to l is $\frac{dv}{dl} = \frac{(1-m)\delta}{\beta}\frac{du}{dl}$. This derivative shows that the variation in predator

population density is influenced by the changes in prey population density. If the prey population decreases, the predator population also decreases. Therefore, fear decreases the individual of prey directly and the predators indirectly.

Impact of prey refuge (m) on prey and predator density

Similarly, as mentioned before, the influence of prey refuge (m) on species density can be analyzed. The dependency of prey population on the refuge parameter is presented below.

$$\left.\frac{du}{dm}\right|_{u=u^*} = -\left.\frac{(u^3\frac{dA_1}{dm}+u^2\frac{dB_1}{dm}+u\frac{dC_1}{dm}+\frac{dL_1}{dm})}{(3A_1u^2+2B_1u+C_1)}\right|_{u=u^*},$$

where, $\frac{dA_1}{dm} = -2bl\delta(1-m)(b_1\beta+c\delta) < 0$, $\frac{dB_1}{dm} = -l\delta(1-m)(2b_1d\beta + (2cd+3p-3mp)\delta) - b(b_1\beta(\beta+b_2l\delta)+\delta(c\beta+a_1l\beta+2b_2cl\delta)) < 0$, $\frac{dC_1}{dm} = b_1(a-d)\beta^2+(ac-d(c+(a_1+b_1b_2)l)-2(1-m)p)\beta\delta-2b_2l(cd+2(1-m)p)\delta^2$, $\frac{dL_1}{dm} = -b_2p\delta(\beta+b_2l\delta) < 0$. Here A_1, B_1, C_1 and L_1 have same meaning as mentioned in Section "Stability analysis". If the coexisting equilibria exist with the condition $C > 0$ and the prey refuge parameter (m) satisfies $0 < m < \frac{R}{S}$, where, $R = b_1d\beta(\beta+b_2l\delta)+\delta((cd+a_1dl+2p)\beta+2b_2l(cd+2p)\delta)-a\beta(b_1\beta+c\delta)$, $S = 2p\delta(\beta+2b_2l\delta)$, then prey density increases as prey refuge increases. Thus, if the prey refuge value increases and lies in a particular range then it leaves positive impact on the prey population for their survival.

Furthermore, we calculate the variation in the predator population relative to prey refuge as $\frac{dv}{dm} = \frac{\delta}{\beta}\left((1-m)\frac{du}{dm}-u\right)$. From this expression, it is obvious that if prey population decreases with respect to prey refuge, i.e., $\frac{du}{dm} < 0$ then $\frac{dv}{dm} < 0$, i.e., predator population decreases. Moreover, if prey population increases, i.e., $\frac{du}{dm} > 0$ then the nature of $\frac{dv}{dm}$, i.e., change in the predator population with respect to prey refuge, will depend on the strength of prey species (u). Thus, if prey refuge increases and lie in a particular range ($0 < m < \frac{R}{S}$) then predator population may increase or decrease according as the strength of prey population.

Stability of spatial model

Our investigation focuses on the spatial behavior of the model (6)–(7) by using a linearized approach around $E_3(u^*, v^*)$:

$$\left.\begin{aligned}\frac{\partial\bar{u}}{\partial t} &= j_{11}\bar{u}+j_{12}\bar{v}+D_1\nabla^2\bar{u},\\ \frac{\partial\bar{v}}{\partial t} &= j_{21}\bar{u}+j_{22}\bar{v}+D_2\nabla^2\bar{v},\end{aligned}\right\} \tag{27}$$

where we add little disturbances $\bar{u} = u-u^*$ and $\bar{v} = v-v^*$. Suppose the solution of the model (27) has the form:

$$\begin{pmatrix}\bar{u}\\ \bar{v}\end{pmatrix} = \begin{pmatrix}l_1\\ l_2\end{pmatrix}\exp(\lambda_k t)\cos(k_x x)\cos(k_y y),$$

where l_1 and l_2 are tiny constants, k_x and k_y specify the wave number components in the x and y directions, and λ_k is the wavelength. The variational matrix of the linearized model (27) is provided as follows:

$$\bar{J} = \begin{pmatrix}j_{11}-D_1k^2 & j_{12}\\ j_{21} & j_{22}-D_2k^2\end{pmatrix}.$$

The wave number, denoted as k, is defined by the equation $k^2 = k_x^2+k_y^2$. The characteristic equation of $\bar{J}$ is

$$\lambda_k^2 - \mathrm{tr}(\bar{J})\lambda_k + \det(\bar{J}) = 0, \tag{28}$$

where, $\mathrm{tr}(\bar{J}) = j_{11}+j_{22}-(D_1+D_2)k^2$, $\det(\bar{J}) = (j_{11}j_{22}-j_{12}j_{21})-(j_{11}D_2+j_{22}D_1)k^2+D_1D_2k^4$.

Theorem 9. *The equilibrium point $E_3(u^*, v^*)$ is locally asymptotically stable in the presence of diffusion if the conditions of Theorem 5 hold.*

Proof. The proof, based on the Routh–Hurwitz criterion, is omitted for brevity. □

Let us now shift our focus to the full picture and consider the complete model (6)–(7).

Theorem 10. *If the equilibrium point $E_3(u^*, v^*)$ of model system (10)–(11) is globally asymptotically stable, the corresponding uniform steady state of model system (6)–(7) is also globally asymptotically stable.*

Proof. To investigate the stability characteristics of this comprehensive system by following [86], we introduce the following function $W_1(t)$, satisfying the property of positive definiteness:

$$W_1(t) = \int\int_\Omega P(u,v)\,dA, \tag{29}$$

where $P(u,v)$ is given in the proof of Theorem 6. Taking derivative of Eq. (29) with respect to time t throughout the solutions of model (6)–(7), we obtain

$$\frac{dW_1}{dt} = I_1+I_2, \tag{30}$$

where

$$I_1 = \int\int_\Omega \frac{dP}{dt}\,dA \quad\text{and}\quad I_2 = \int\int_\Omega\left(D_1\frac{\partial P}{\partial u}\nabla^2u+D_2\frac{\partial P}{\partial v}\nabla^2v\right)dA.$$

Using Green's first identity in the plane

$$\iint_\Omega F_1\nabla^2F_2\,dA = \int_{\partial\Omega}F_1\frac{\partial F_2}{\partial n}\,ds - \iint_\Omega\left(\nabla F_1.\nabla F_2\right)\,dA,$$

where, $\frac{\partial F_2}{\partial n}$ is the directional derivative in the direction of the unit outward normal to $\partial\Omega$ and s is the arc length. Then with $F_1 = \frac{\partial P}{\partial u}$ and $F_2 = u$, we obtain,

$$\int\int_\Omega\frac{\partial P}{\partial u}\nabla^2u\,dA = \int_{\partial\Omega}\frac{\partial P}{\partial u}\frac{\partial u}{\partial n}\,ds - \int\int_\Omega\frac{\partial^2P}{\partial u^2}\left[\left(\frac{\partial u}{\partial x}\right)^2+\left(\frac{\partial u}{\partial y}\right)^2\right]dA \le 0.$$

Since $\frac{\partial u}{\partial n} = 0$ and $\frac{\partial^2P}{\partial u^2} > 0$, we obtain

$$\int\int_\Omega\frac{\partial P}{\partial u}\nabla^2u\,dA = -\int\int_\Omega\frac{\partial^2P}{\partial u^2}\left[\left(\frac{\partial u}{\partial x}\right)^2+\left(\frac{\partial u}{\partial y}\right)^2\right]dA \le 0.$$

Similarly if we take $F_1 = \frac{\partial P}{\partial v}$ and $F_2 = v$, we obtain,

$$\int\int_\Omega\frac{\partial P}{\partial v}\nabla^2v\,dA = \int_{\partial\Omega}\frac{\partial P}{\partial v}\frac{\partial v}{\partial n}\,ds - \int\int_\Omega\frac{\partial^2P}{\partial v^2}\left[\left(\frac{\partial v}{\partial x}\right)^2+\left(\frac{\partial v}{\partial y}\right)^2\right]dA \le 0,$$

also as $\frac{\partial u}{\partial n} = 0$ and $\frac{\partial^2P}{\partial u^2} > 0$, we have

$$\int\int_\Omega\frac{\partial P}{\partial v}\nabla^2v\,dA = -\int\int_\Omega\frac{\partial^2P}{\partial v^2}\left[\left(\frac{\partial v}{\partial x}\right)^2+\left(\frac{\partial v}{\partial y}\right)^2\right]dA \le 0.$$

This indicates that I_2 is less than or equal to zero. From above, we note that if $I_1 \le 0$, then $\frac{dP}{dt} \le 0$. This implies that if in the absence of diffusion, E_3 is globally asymptotically stable, then in the presence of diffusion, E_3 will remain globally asymptotically stable. □

Turing instability

We know that there are two conditions for the emergence of Turing patterns. Firstly, the equilibrium point remains stable under spatial uniform disturbance (i.e. without considering spatial diffusion); secondly,

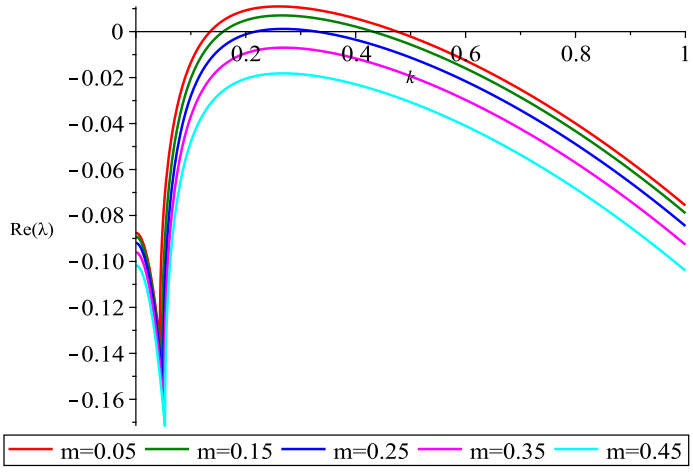

Fig. 1. Dispersion diagram of model (1)–(2) with specific values assigned to the parameter m. The values of relevant parameters are, $a = 0.6$, $d = 0.01$, $b = 0.1$, $l = 0.8$, $p = 0.2$, $c = 0.5$, $b_1 = 1$, $a_1 = 0.025$, $\delta = 0.2$, $\beta = 0.016$, $b_2 = 0.025$. The diffusion coefficients are $D_1 = 0.1$ and $D_2 = 50$, respectively.

under the spatial non-uniform disturbance (i.e. considering spatial diffusion), the equilibrium point exists in unstable mode, that is, there is an eigenvalue whose real part is positive. Here, we study the conditions under which Turing patterns can be generated at the positive equilibrium point $E_3(u^*, v^*)$: (i) $j_{11} + j_{22} < 0$; (ii) $j_{11}j_{22} - j_{12}j_{21} > 0$; (iii) $\frac{j_{11}D_2 + j_{22}D_1}{2D_1D_2} > 0$; (iv) $(j_{11}D_2 + j_{22}D_1)^2 > 4D_1D_2det(J)$. Due to the difficulty in calculating the specific expression of $E_3(u^*, v^*)$ and the algebraic complexity of its eigenvalues, we cannot further obtain more specific conditions. Therefore, to gain further insights, we employ computer-aided numerical simulation for a comprehensive analysis and obtain the dispersion diagram of system (1)–(2) (Fig. 1). We can find that the real part of the eigenvalue gradually increases with the decrease of parameter m in the suitable range of parameters. Turing patterns emerge when the real part is positive.

Turing instability of spatial system with cross diffusion

Next, the influence of cross diffusion on model system (10)–(11) is considered, and the model adopted is as follows:

$$\frac{\partial u}{\partial t} = \frac{au}{1+lv} - du - bu^2 - \frac{p(1-m)uv}{cv + b_1(1-m)u + a_1} + D_{11}\nabla^2 u + D_{12}\nabla^2 v, \quad (31)$$

$$\frac{\partial v}{\partial t} = \delta v - \frac{\beta v^2}{(1-m)u + b_2} + D_{21}\nabla^2 u + D_{22}\nabla^2 v, \quad (32)$$

with initial restrictions

$$u(x, y, 0) > 0, \quad v(x, y, 0) > 0, \quad \text{for } (x, y) \in \Omega, \quad (33)$$

and boundary conditions

$$\frac{\partial u}{\partial n} = \frac{\partial v}{\partial n} = 0, \ (x, y) \in \partial\Omega \ \text{ for all } t, \quad (34)$$

where D_{11} and D_{22} are self diffusion rate coefficient of prey and predator, respectively. D_{12} and D_{21} are cross diffusion rate coefficient, respectively. D_{12} represents the tendency of the prey to evade predators and D_{21} quantifies the predator's predatory behavior towards the prey. The value of D_{12} and D_{21} may be positive or negative. If the diffusion coefficient is positive it means the population spreads from areas of high concentration to areas of low concentration, conversely, a negative diffusion coefficient signifies net movement against the concentration gradient, from low to high density regions. The remaining parameters are defined in the same way as for model system (6)–(7). Next, we linearize the model and analyze (31)–(32) at $E_3(u^*, v^*)$ in the following way:

$$\frac{\partial \tilde{u}}{\partial t} = j_{11}\tilde{u} + j_{12}\tilde{v} + D_{11}\nabla^2\tilde{u} + D_{12}\nabla^2\tilde{v}, \quad (35)$$

$$\frac{\partial \tilde{v}}{\partial t} = j_{21}\tilde{u} + j_{22}\tilde{v} + D_{21}\nabla^2\tilde{u} + D_{22}\nabla^2\tilde{v}, \quad (36)$$

where, we introduce slight disturbances to the system $\tilde{u} = u - u^*$ and $\tilde{v} = v - v^*$. The model (31)–(32) has a solution of the following form

$$\tilde{u}(r, t) = \alpha e^{\lambda t + ikr}, \quad (37)$$

$$\tilde{v}(r, t) = \beta e^{\lambda t + ikr}, \quad (38)$$

where k is the wave number, α and β are sufficiently small constants and λ is wave length. The Jacobian matrix of model (31)–(32) is

$$\tilde{J} = \begin{pmatrix} j_{11} - D_{11}k^2 & j_{12} - D_{12}k^2 \\ j_{21} - D_{21}k^2 & j_{22} - D_{22}k^2 \end{pmatrix}.$$

The characteristic equation of $\tilde{J}$ is written as

$$\lambda^2 - \mathrm{tr}(\tilde{J})\lambda + \det(\tilde{J}) = 0, \quad (39)$$

where, $\mathrm{tr}(\tilde{J}) = j_{11} + j_{22} - (D_{11} + D_{22})k^2$, $\det(\tilde{J}) = (j_{11}j_{22} - j_{12}j_{21}) - (j_{11}D_{22} + j_{22}D_{11} - j_{12}D_{21} - j_{21}D_{12})k^2 + (D_{11}D_{22} - D_{12}D_{21})k^4$. Therefore, the necessary conditions for Turing patterns to be generated at equilibrium point $E_3(u^*, v^*)$ are (i) $j_{11} + j_{22} < 0$; (ii) $j_{11}j_{22} - j_{12}j_{21} > 0$; (iii) $j_{11}D_{22} + j_{22}D_{11} - j_{12}D_{21} - j_{21}D_{12}) > 0$; (iv) $(j_{11}D_{22} + j_{22}D_{11} - j_{12}D_{21} - j_{21}D_{12})^2 > 4(D_{11}D_{22} - D_{12}D_{21})det(J)$. Because of the intricate algebraic nature of equilibrium points and eigenvalues, the critical values for the emergence of Hopf bifurcations and Turing branches cannot be visually presented here. Numerical approaches are used to analyze the Turing region as depicted in Fig. 11. Region I exhibits an unstable solution, leading to Turing instability. All solutions in area II are stable. Hopf instability is present in area III, while Turing–Hopf instability is present in region IV (see Fig. 2).

Numerical results

Building upon the theoretical analysis of the predator–prey model, this section presents numerical simulations of both the non-spatial and spatial models. Fig. 3(a) shows that when we have moderate level of fear and refuge then two coexisting equilibria exist. Also, if prey refuge values crosses a level then coexisting states reduce from two to one (see Fig. 3(b)). Further, if the fear level becomes high then the coexistence of species is not possible (see Fig. 3(c)).

Non-spatial model

In Fig. 4(a), $\delta = 0.01$, the solution curves approach a stable coexistence $(0.2856, 0.1861)$. In Fig. 4(b), as intrinsic growth rate of predator δ increases from 0.01 to 0.03 then these solution curves oscillates around

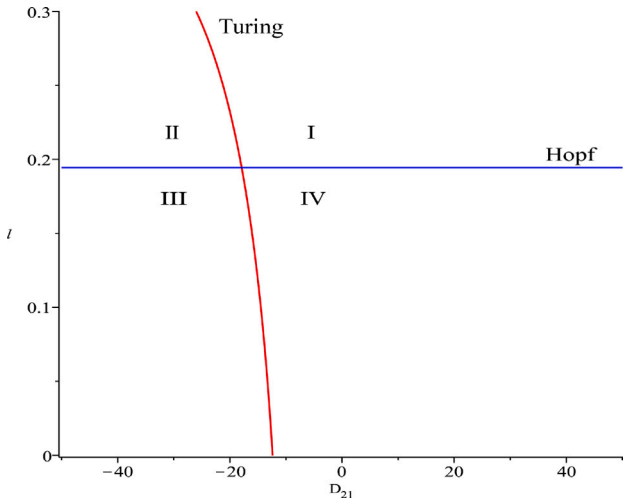

Fig. 2. Diagram depicting bifurcation of model (31)–(32) in $D_{21} - l$ parameter plane. The values of ecosystem parameters are, $a = 0.6$, $d = 0.01$, $b = 0.1$, $p = 0.2$, $c = 0.5$, $b_1 = 1$, $a_1 = 0.025$, $\delta = 0.2$, $\beta = 0.016$, $b_2 = 0.025$. The diffusion coefficients are $D_{11} = 0.8$, $D_{12} = -0.4$ and $D_{22} = 1$.

the equilibrium point $(0.0786, 0.1741)$. Additionally, as intrinsic growth rate δ become $\delta = 0.06$ then the system exhibits a tendency towards the absence of prey, converging on the state where prey population is zero $(0, 0.0563)$, as shown in Fig. 4(c). Fig. 4(d) is the phase portrait corresponding to Fig. 4(b). Thus, the intrinsic growth rates play a very vital role to make the system stable, oscillatory and prey free.

Spatial model

With the aim of understanding how the system behaves over time and space, we present the spatial distribution patterns of prey and predator species in this section, generated using computer numerical simulations. This simulations utilize the approach of backward finite difference, the study area is a 200×200 grid, and its boundary satisfies Neumann boundary conditions. The space step size is $\Delta h = 2$, and the time step size is $\Delta t = 0.1$. The choice of initial restrictions is a recognized determinant of the system's dynamic behavior. For the purpose of obtaining the spatiotemporal dynamics of the nontrivial equilibrium, we begin by initializing the system with a small, random perturbation near the non-trivial equilibrium point. In the numerical simulation, our analysis reveals that the spatial distribution patterns of both prey and predator populations exhibit the same characteristics. For the sake of clarity and conciseness, only the spatial distribution of the prey population is depicted here. Moreover, from system (6), we recognize parameter l representing the fear effect, while parameter m embodies the concept of refuge for the prey. In light of these established relationships, this study delved into exploring the impact of parameters l and m on the spatial distribution of the prey species.

Effect of the fear factor l

The investigation of the fear factor's influence on the prey's spatial distribution involved systematically changing only parameter l, while holding all remaining model parameters fixed. Therefore, we chose six different parameter values to simulate the spatial distribution of prey (Fig. 7). Fig. 7 shows the spatial distribution of prey species under different fear factors. The investigation demonstrates that as the fear factor (l) increases, the overall spatial distribution pattern of the prey population remains largely unchanged, retaining its characteristic spot pattern structure. However, results indicate a gradual rise in the maximum value and a gradual decline in the minimum value of the prey population's density function. That is, the density difference between the prey populations is increasing (see Fig. 8). In addition, we also examined the behavior of the prey population by analyzing the changes in its average density. (see Fig. 9a). Our analysis reveals that the average density of the prey population exhibits a tendency towards stability over time. However, an increase in the fear factor (parameter l) is accompanied by a gradual rise in the average density. However, results indicate that beyond a certain level, further amplification of the fear factor (l) leads to a gradual decrease in the average prey density (see Fig. 9b). This suggests that appropriate fear is beneficial for prey survival, while too much fear factor will inhibit prey survival.

Effect of the refuge m

In Fig. 10, we show the corresponding changes of the spatial pattern of the prey population at different level of refuges, $m = 0.05, 0.15, 0.2, 0.25$. The simulation results show that with the change of parameter m, although there is no significant difference in the pattern structure, there is a notable disparity in the average density of the prey population. The time series diagram (Fig. 11) shows that the average density of the prey population eventually stabilizes over time. Additionally, a positive correlation is observed between the average prey density and the refuge value (parameter m).

Beddington–DeAngelis functional response

Here, we explore how variations in certain parameters of the Beddington–DeAngelis functional response impact the spatial distribution of the prey species. Fig. 12 shows the effect of mutual interference parameter (b_1) between prey species on the pattern structure of the prey population. We also obtain that when the disturbance between predator species is small, the spatial distribution of the prey population is a spot pattern. A slight increase in the intensity of intra-predator disturbance results in a transformation of the prey population's spatial distribution from a purely spot-patterned form to a mixed pattern exhibiting both spots and stripes. Further analysis reveals that with a continuous rise in the intensity of intra-predator interactions, the prey population's spatial distribution transition through various stages, eventually converging towards a stable stripe pattern.

In Fig. 13, we simulate the effect of the change of parameter a_1 (half saturation constant) on the spatial distribution of the prey population. The analysis uncovers the fact that in case of the gradual increase in the parameter a_1, the prey population always maintains a spot pattern structure. When parameter a_1 continues to increase, the prey population finally presents a uniform distribution. That is when half saturation constant crosses a threshold value and continue to increase then the distribution of prey density is constant.

Effect of cross diffusion on the spatial pattern of the population

Our investigation focused on elucidating the effects of cross diffusion on the spatial distribution of the prey population. We achieved this by systematically modifying the values of parameters D_{12} and D_{21}, while keeping all other parameters constant. Therefore, three different parametric values were selected to simulate the spatial distribution of prey species (see Figs. 14 and 15). Our investigation revealed minimal alterations in the spatial distribution patterns of the prey species despite increasing the rate at which they avoid predators (refer Fig. 14). However, results indicate a gradual rise in the maximum value and a gradual decline in the minimum value of the prey population's density. However, as depicted in Fig. 15, the highest prey population density steadily decreased, while the lowest density gradually increased with the increase in the predator's pursuit rate. Also the pattern structure of prey population did not change significantly. Although appropriate fear is beneficial to the survival of prey, the prey density will decrease when the predator chases the prey at a high rate, as shown in Fig. 15 a and b. In other words, our findings suggest that the effectiveness of the

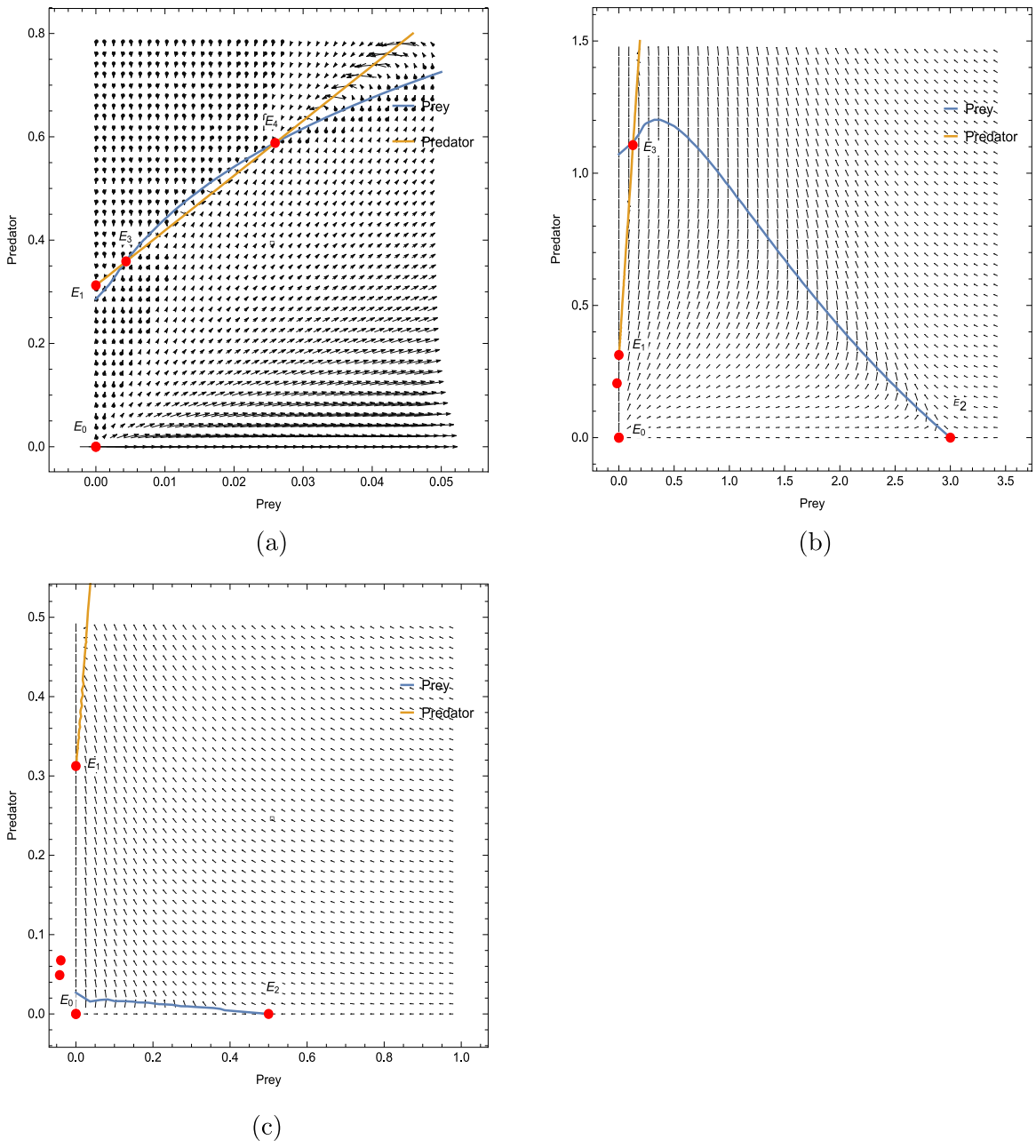

Fig. 3. Possible number of equilibria under different values of fear factor (l) and prey refuge parameter (m). (a) There are two coexisting equilibria E_3 and E_4 for $m = 0.15$ and $l = 0.45$. (b) As the prey refuge parameter varies from $m = 0.15$ to $m = 0.5$ keeping all other parameters unchanged, there is only one equilibrium E_3. (c) Further, as the fear factor increases from $l = 0.45$ to $l = 3.8$ keeping all other parameters unchanged as in Fig. 3(b), no coexisting equilibria exist. In all three figures, three boundary equilibria E_0, E_1, E_2 always exist. All other parametric values are $a = 0.6$, $d = 0.3$, $b = 0.1$, $p = 0.15$, $c = 0.5$, $b_1 = 6$, $a_1 = 0.01$, $\delta = 0.2$, $\beta = 0.016$, $b_2 = 0.015$.

fear response in enhancing prey survival diminishes as the predator's chasing tendency becomes more pronounced.

Conclusion

The prey-predator relationship is formulated when prey are exposed to predators, leading to a decrease in the prey population due to this interaction. If prey biomass is exceedingly low, the predator population is likely to starve. Therefore, a reduction in the predator biomass is accompanied by a decrease in prey consumption. The population of prey grows in this scenario. In addition to direct interaction, the indirect killing factor influences the growth of the prey. Our analysis reveals that both the fear factor and the availability of refuge significantly influence the dynamical behavior of the prey population, leading to substantial effects on the system's behavior.

This paper presents an investigation of a spatial prey-predator system incorporating self-diffusion, which also include the indirect predation feature. The main focus of this work is to examine how the presence of refuges for prey and the fear they experience due to predation affect the population dynamics within the predator–prey model. The model incorporates the Beddington–DeAngelis functional response to represent the predator's consumption of the prey biomass. We have examined the model (6)–(7) without self-diffusion, in a non-spatial context. We have also examined the system with self-diffusion in a spatial context. We have demonstrated that the suggested model system for non-spatial systems (10)–(11) is biologically meaningful by showing that its solutions are positive and bounded. Four types of

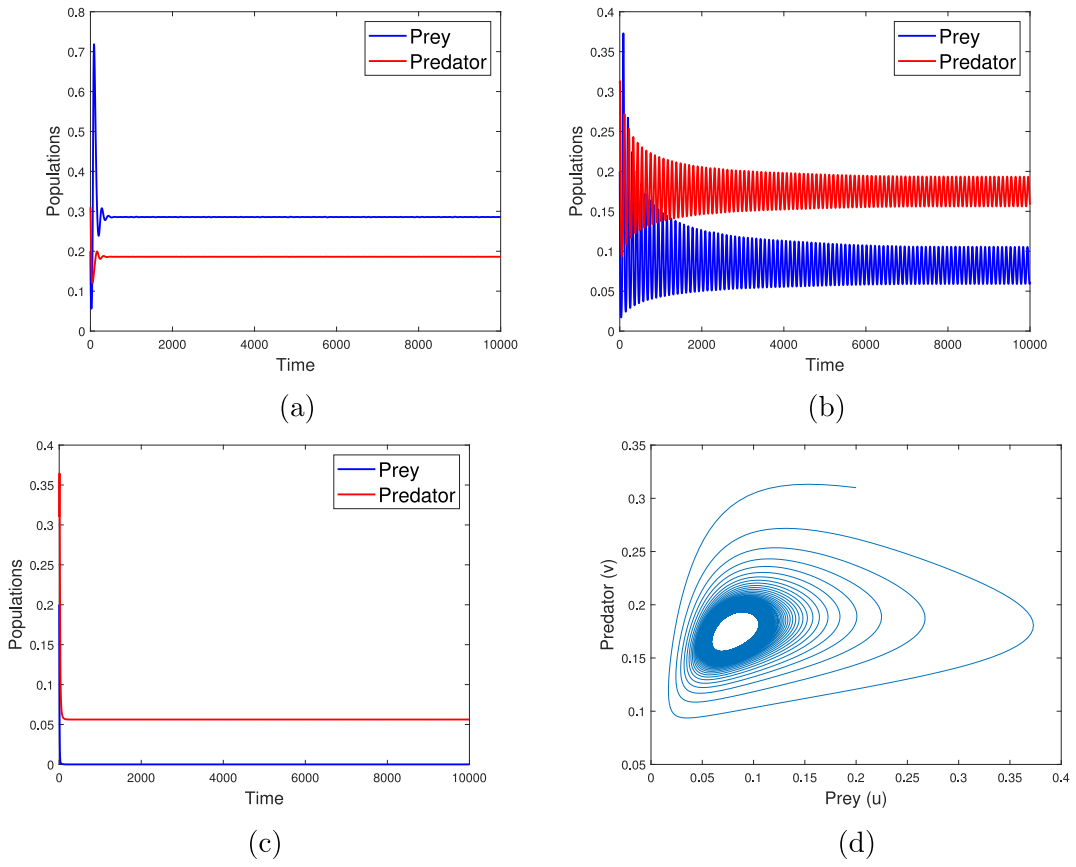

Fig. 4. Solution curves of model (10)–(11). Here, we vary the parameter of Hopf bifurcation (δ), assuming all other ecosystem parameter values: $a = 0.6$, $d = 0.3$, $p = 0.15$, $b = 0.1$, $b_1 = 6$, $a_1 = 0.01$, $c = 0.5$, $m = 0.01$, $\beta = 0.016$, $b_2 = 0.015$, $l = 4$.

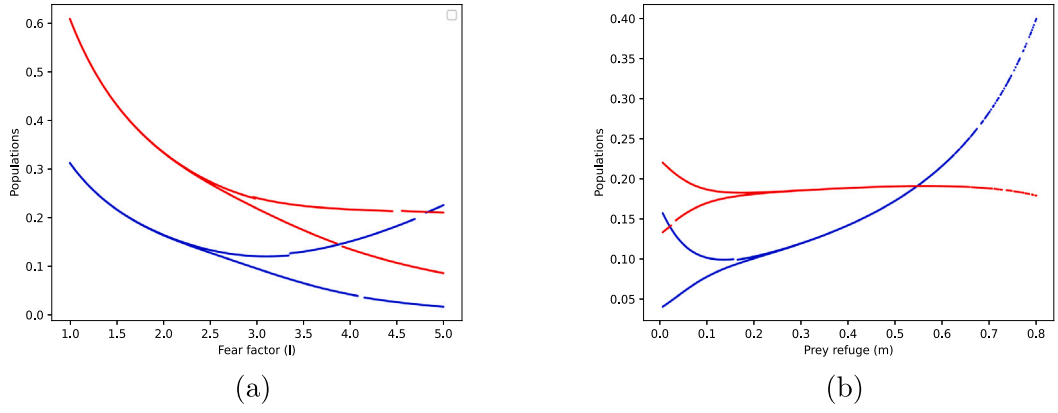

Fig. 5. Plots of numerical simulation results with parametric values: $a = 0.6$, $d = 0.3$, $\beta = 0.016$, $p = 0.15$, $b = 0.1$, $\delta = 0.03$, $b_1 = 6$, $a_1 = 0.01$, $c = 0.5$, $b_2 = 0.015$. Here, the blue and red curves depict the prey and predator population, respectively. **(a)** Bifurcation diagrams with reference to l for $m = 0.01$. The dividing of line represent the transition from steady point solution to oscillatory dynamics. In this bifurcation, we obtain a steady state to limit cycle transition (supercritical Hopf bifurcation). **(b)** Bifurcation diagrams with respect to m for $l = 4$. Here, oscillatory dynamics tends to a steady state i.e., limit cycle to steady state via sub-critical Hopf bifurcation. (For interpretation of the references to color in this figure legend, the reader is referred to the web version of this article.)

equilibria were identified when investigating the dynamics of system (10)–(11). Prey-free equilibria exist when the intrinsic growth rate of the predator biomass is positive, while predator-free equilibria exist when the growth rate of the prey biomass exceeds the natural death rate. There can be a maximum of two coexisting equilibria based on the parametric limitations outlined in Section "Stability analysis". The number of coexisting states is closely linked to the fear factor and prey refuge parameters. By adjusting these control settings, one can achieve the coexistence of states ranging from zero to two, as shown in Fig. 3.

Furthermore, our investigation focused on the stability of the identified equilibria. Theorems 4 and 5 elucidate the influence of fear factor and prey refuge on the stability of prey free and coexisting equilibria, respectively. We examined the global stability properties of the coexisting equilibria within the model, taking into account the boundaries of the parameter space. An optimal combination of prey refuge and fear factor values can ensure global stability of the system governed by Eqs. (3) and (4) as stated in Theorem 6. We conducted a Hopf-bifurcation analysis based on the intrinsic growth rate of the predator species (δ). A key outcome of this study is the development

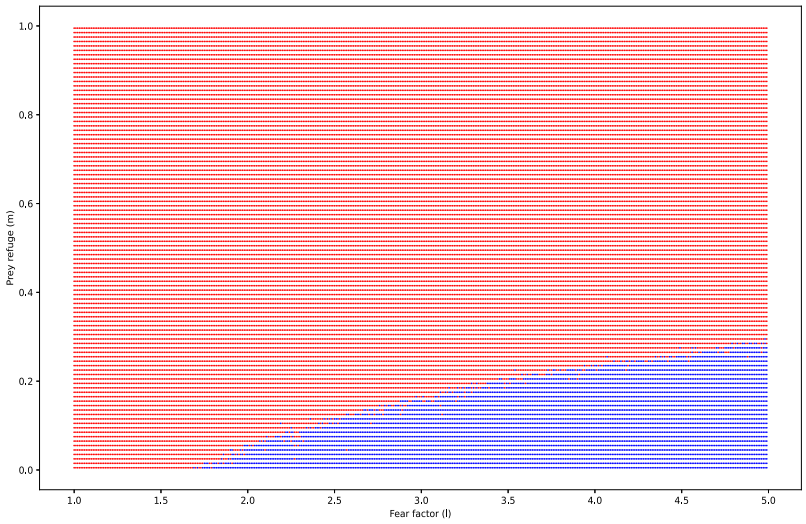

Fig. 6. $l-m$ parameter space. Graph depicting numerical simulation outcomes of the model (10)–(11) with parametric values: $a = 0.6$, $d = 0.3$, $\beta = 0.016$, $p = 0.15$, $b = 0.1$, $\delta = 0.03$, $b_1 = 6$, $a_1 = 0.01$, $c = 0.5$, $b_2 = 0.015$. In this diagram, the red region indicates parameter values for fear factor (l) and prey refuge (m) that lead to a stable, unchanging population (steady state). Conversely, the blue region represents parameter combinations where prey and predator populations fluctuate over time (oscillatory state). (For interpretation of the references to color in this figure legend, the reader is referred to the web version of this article.)

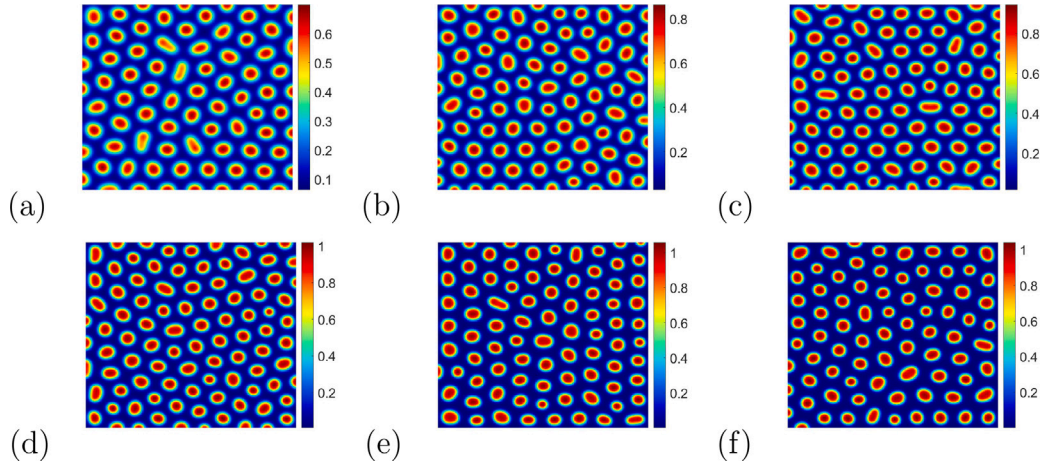

Fig. 7. Spatial pattern depicting prey species under different fear factor l. (a) $l = 0.4$; (b) $l = 0.5$; (c) $l = 0.6$; (d) $l = 0.8$; (e) $l = 0.9$; (f) $l = 1.2$. The remaining parameter values are, $a = 0.6$, $d = 0.01$, $b = 0.1$, $m = 0.15$, $p = 0.2$, $c = 0.5$, $b_1 = 1$, $a_1 = 0.025$, $\delta = 0.2$, $\beta = 0.016$, $b_2 = 0.025$.

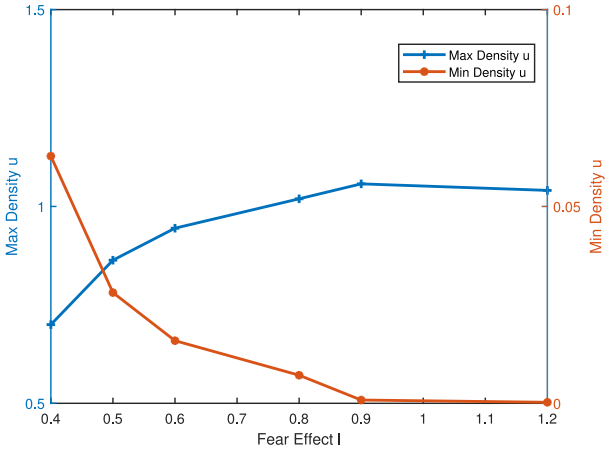

Fig. 8. The trends of maximum and minimum densities of prey species under different levels of fear l. The values of relevant parameters are mentioned in Fig. 7.

of a formula that allows for the computation of the critical value of (δ) triggering a Hopf bifurcation and the associated alteration in the system's stability characteristics. Further the transcritical bifurcation for non-spatial system has been analyzed. In the context of our model, the ecological aspect for transcritical bifurcation is that the prey refuge and fear effects modify the effective growth rate of the prey populations. If prey refuge becomes more effective, it can simulate a lower growth rate for the prey from the predators perspective, potentially preventing the prey population from reaching a critical growth threshold. Moreover, fear effects can reduce the effective prey growth rate by impacting their foraging and reproductive behaviors, also influence when and how a transcritical bifurcation might occur. So identifying and understanding the critical growth rate thresholds that lead to significant changes in the stability and dynamics of prey-predator interactions. The influence of prey refuge and fear factor has been investigated for the non-spatial system. The fear response of prey species has a direct detrimental influence on prey population under some conditions and indirectly decreases the predator biomass. If the prey refuge is within the range of $0 < m < R/S$(where R and S have the same meaning as in Section "Impact of prey refuge (m) on prey and predator density"), it positively affects the prey population. Changes in the strength of the prey population exert

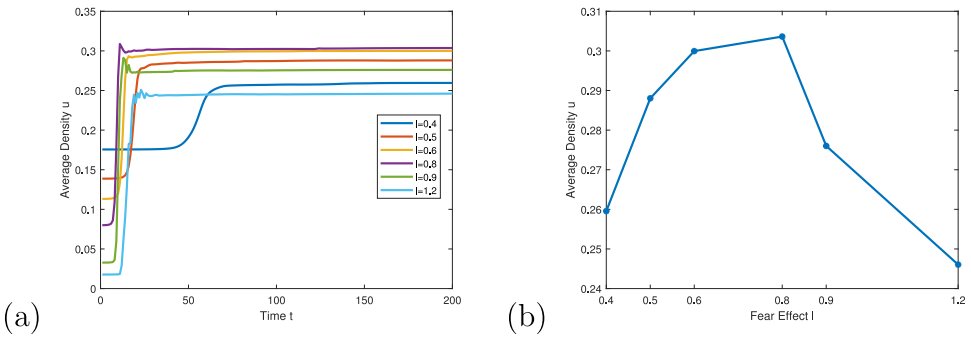

Fig. 9. The average density of prey species under different fear factors l. The values of relevant parameters are shown in Fig. 7.

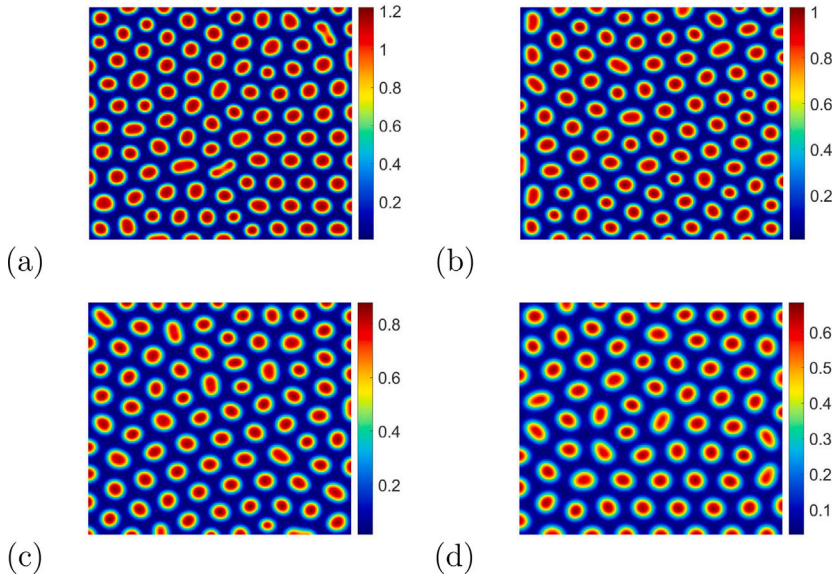

Fig. 10. Spatial pattern depicting prey species for different values of prey refuge parameter m. (a) $m = 0.05$; (b) $m = 0.15$; (c) $m = 0.2$; (d) $m = 0.25$. The other parametric values are $a = 0.6$, $d = 0.01$, $b = 0.1$, $l = 0.8$, $p = 0.2$, $c = 0.5$, $b_1 = 1$, $a_1 = 0.025$, $\delta = 0.2$, $\beta = 0.016$, $b_2 = 0.025$.

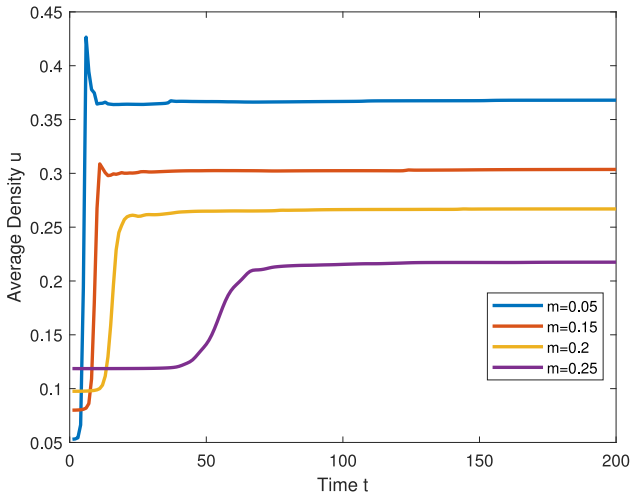

Fig. 11. The average density of prey species for different values of m. The values of relevant parameters are shown in Fig. 10.

a significant influence on the predator population, leading to potential increases/decreases in predator abundance.

Through numerical simulations, we investigated the long-term dynamics of the system. We observed that a small adjustment to the predator's intrinsic growth rate can be a tipping point, causing the system to switch from a stable state to a cyclical pattern (Fig. 4). Fig. 5 displays the system's shift from a stable state to an oscillatory state based on variations in m and l. Fig. 6 indicates the relationship between the fear factor level and prey refuge range that can stabilize the system described by Eqs. (10)–(11) through the suitable selection of parameters m and l. The dynamics of predator–prey interactions are significantly influenced by the availability of refuges for prey, encompassing both physical shelters (spatial refuges) and temporary safety measures (temporal refuges). Additionally, prey behavior plays a crucial role, with strategies such as forming aggregations or reducing their activity levels (refuge) contributing to a decrease in predation risk [80,87].

In Fig. 1, the dispersion diagram of eigenvalue with respect to prey refuge (m) shows that when the value of m decreases, the real part of eigenvalue increases. Fig. 3 shows the impact of prey refuge (m) and fear effect (l). By changing the values of both the parameters, one can have different number of steady states. Our findings emphasizes the significant influence of refuge on the dynamic characteristics of predator–prey interactions.

Further, the investigation centers on the dynamics of the model under conditions that include diffusion. We have discussed the stability of spatial model system (6)–(7). Turing stability has been performed numerically. From numerical simulation, we have observed that fear

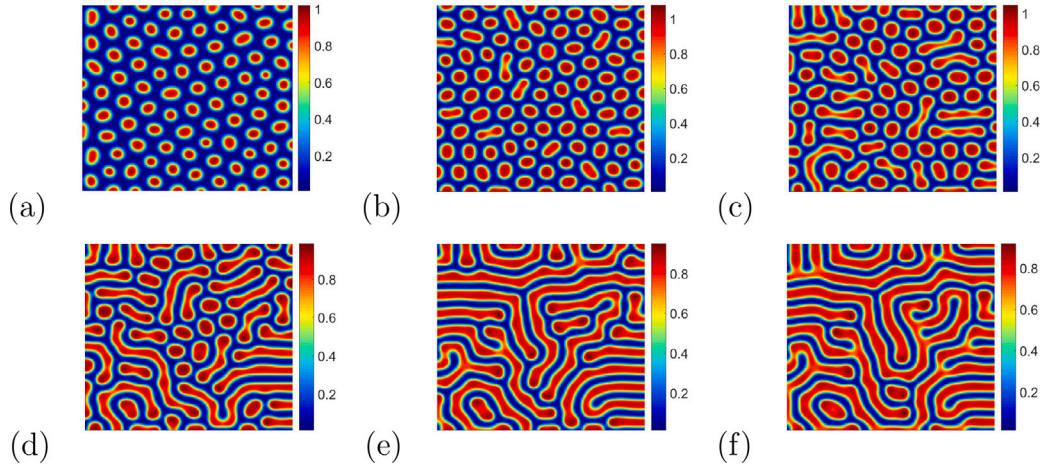

Fig. 12. The spatial distribution corresponding to prey species with the change of parameter b_1. (a) $b_1 = 1$; (b) $b_1 = 2$; (c) $b_1 = 3$; (d) $b_1 = 4$; (e) $b_1 = 5$; (f) $b_1 = 6$. Here $m = 0.15$, $l = 0.8$. All other parameters retain the values used in the previous analysis.

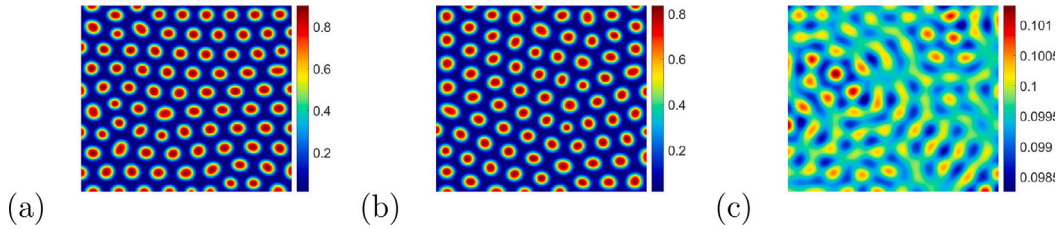

Fig. 13. The spatial distribution corresponding to prey species along with the change of parameter a_1. (a) $a_1 = 0.065$; (b) $a_1 = 0.085$; (c) $a_1 = 0.105$. The remaining parameters retain their previously assigned values for this simulation.

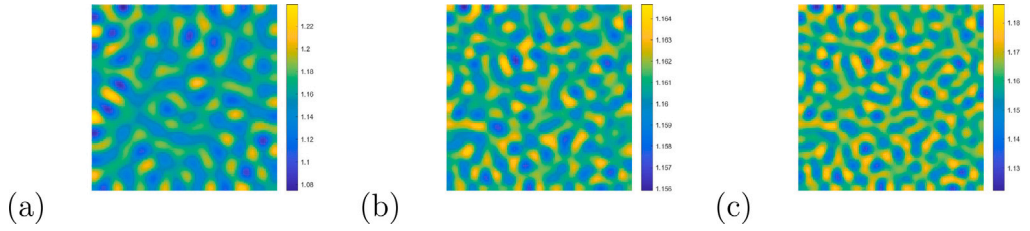

Fig. 14. The spatial distribution corresponding to prey species with the change of parameter D_{12}. (a) $D_{12} = -0.3$; (b) $D_{12} = -0.5$; (c) $D_{12} = -0.7$. Here $m = 0.15$, $l = 0.8$, $b_1 = 1$, $a_1 = 0.025$. No changes were made to the other parameters compared to the earlier investigation.

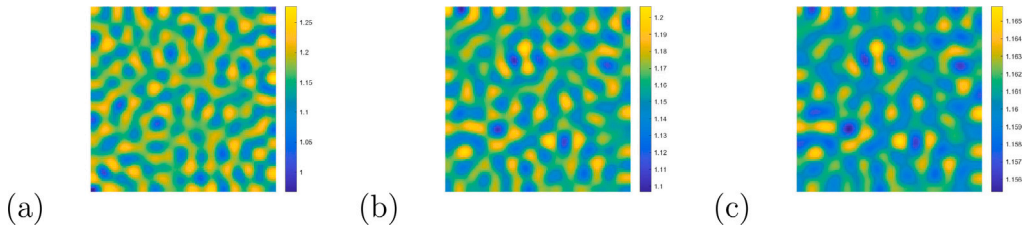

Fig. 15. The spatial distribution corresponding to prey species with respect to the parameter D_{21}. (a) $D_{21} = 0.1$; (b) $D_{21} = 0.8$; (c) $D_{21} = 1.5$. Here $m = 0.15$, $l = 0.8$, $b_1 = 1$, $a_1 = 0.025$. No changes were made to the other parameters compared to the earlier investigation.

effect, prey refuge have great impact on the spatial dynamics of model. The analysis indicates that the level of fear plays a crucial role in prey population dynamics, with a balanced fear response promoting survival and an extreme response hindering it. Further, from time series diagram (Fig. 11), we have concluded that the average density of the prey finally moves to a stable state with respect to time. As the refuge value m increases, the average prey density exhibits a corresponding increase. Also, we have obtained that density distribution of species is in form of spot and stripe like patterns. Further, we have found that mutual interference between prey is also play an important role for pattern formation. With the gradual increase of the parameter b_1, the spatial distribution of the prey varies from spot pattern to spot and stripe mixed pattern to strip pattern, and the pattern structure gradually changes. Moreover, when the half saturation constant parameter continues to increase, the prey population eventually depicts an uniform distribution (Fig. 13).

Future Directions: There may be quantitative and qualitative changes in the spatio-temporal patterns as a result of parameter variation. In

Table 2
A comparative analysis of the proposed model (6)–(7) with existing model.

Existing models	Model description	Conclusion
Han et al. [80]	Cross-diffusion driven pattern formation and selection in a modified Leslie–Gower predator–prey model with fear effect	A high cross-diffusion rate of predators can lead to stripe patterns, while a low rate can induce spot patterns. Intermediate rates can result in a mixture of spot and stripe patterns. The fear factor significantly influences the spatially heterogeneous distribution of the two species.
Guin et al. [82]	Pattern dynamics of a reaction–diffusion predator–prey system with both refuge and harvesting	Linear prey harvesting deviations also exhibit stripe patterns and a mixture of stripes and labyrinthine patterns within a certain range of prey refuge. This complex dynamic phenomenon includes Turing pattern behaviors.
Souna et al. [88]	Spatiotemporal behavior in a predator–prey model with herd behavior and cross-diffusion and fear effect	Spot, strip-spot and strip patterns are obtained w.r.t. cross-diffusion rates for the predators. The cross-diffusion rate and the prey herd play vital role in the existence of Turing bifurcation.
Our proposed study	A modified Holling Tanner model system : the role of prey refuge and fear effect	In the absence of self-diffusion, the system undergoes Hopf bifurcation and transcritical bifurcation. With the presence of self-diffusion, an optimal level of fear promotes prey survival, while excessive fear hinders prey survival. Increasing mutual interference among prey shifts the spatial density distribution from a spot-like pattern to a mixture of stripes and spots, eventually transition to a stripe-like pattern. The distribution of prey populations remains constant with increasing semi saturation. In the presence of cross-diffusion, when prey is significantly impacted by predator pursuit, the beneficial effect of fear on prey survival is limited. The prey refuge affects the spatial distribution and stability of the system.

many instances, it would not be basically dismissed and it is worth explaining and developing. Additionally, there are lot of scope for further exploration regarding this issue. Further exploration of this interacting model incorporating other relevant biological effects, such as the influence of external periodic forces and spatial noise, is warranted. These issues will systematically be addressed in future studies (see Table 2).

CRediT authorship contribution statement

Deepak Tripathi: Conceptualization, Methodology, Software, Investigation, Writing – review & editing. **Jai Prakash Tripathi:** Investigation, Writing – review & editing. **Satish Kumar Tiwari:** Investigation, Writing – review & editing. **Debaldev Jana:** Investigation, Writing – review & editing. **Li-Feng Hou:** Investigation, Writing – review & editing. **Yu Shi:** Investigation, Writing – review & editing. **Gui-Quan Sun:** Investigation, Writing – review & editing. **Vandana Tiwari:** Investigation, Writing – review & editing. **Joshua Kiddy K. Asamoah:** Investigation, Writing – review & editing.

Declaration of competing interest

The authors declare that they have no known competing financial interests or personal relationships that could have appeared to influence the work reported in this paper.

Data availability

The data that supports the findings of this study are available within the article.

Acknowledgments

This research is financially supported by the National Key Research and Development Program of China (Grant No. 2018YFE0109600) and the National Natural Science Foundation of China (Grant Nos. 42075029). This work is supported by a grant from the Science and Engineering Research Board (SERB), India, awarded to Jai Prakash Tripathi [File No. ECR/2017/002786] and [File No. MTR/2022/001028]. The research work of Satish Kumar Tiwari has been supported by RGIPT, Jais, Amethi, India.

References

[1] Pal S, Pal N, Samanta S, Chattopadhyay J. Effect of hunting cooperation and fear in a predator–prey model. Ecol Complex 2019;39:100770. http://dx.doi.org/10.1016/j.ecocom.2019.100770.
[2] Elizabeth Maczulak A. Biodiversity: conserving endangered species. Infobase Publishing; 2010.
[3] Fletcher AL. Mendel's ark: Biotechnology and the future of extinction. Springer; 2014.
[4] Cresswell W. Predation in bird populations. J Ornithol 2011;152:251–63. http://dx.doi.org/10.1007/s10336-010-0638-1.
[5] Creel S, Christianson D. Relationships between direct predation and risk effects. Trends Ecol Evol 2008;23:194–201. http://dx.doi.org/10.1016/j.tree.2007.12.004.
[6] Lima SL. Nonlethal effects in the ecology of predator–prey interactions. Bioscience 1998;48:25–34. http://dx.doi.org/10.2307/1313225.
[7] Lima SL. Predators and the breeding bird: behavioral and reproductive flexibility under the risk of predation. Biol Rev 2009;84:485–513. http://dx.doi.org/10.1111/j.1469-185X.2009.00085.x.
[8] Creel S, Christianson D, Liley S, Jr. JAW. Predation risk affects reproductive physiology and demography of elk. Science 2007;315:960. http://dx.doi.org/10.1126/science.1135918.
[9] Svennungsen TO, Holen ØH, Leimar O. Inducible defenses: continuous reaction norms or threshold traits? Amer Nat 2011;178:397–410. http://dx.doi.org/10.1086/661250.
[10] Peacor SD, Peckarsky BL, Trussell GC, Vonesh JR. Costs of predator-induced phenotypic plasticity: a graphical model for predicting the contribution of nonconsumptive and consumptive effects of predators on prey. Oecologia 2013;171:1–10. http://dx.doi.org/10.1007/s00442-012-2394-9.
[11] Tripathi Jai Prakash, et al. Cannibalistic enemy–pest model: effect of additional food and harvesting. J Math Biol 2023;87(4):58. http://dx.doi.org/10.1007/s00285-023-01991-9.
[12] Liang J, Liu C, Sun GQ, Li L, Zhang L, Hou M, Wang H, Wang Z. Nonlocal interactions between vegetation induce spatial patterning. Appl Math Comput 2022;428:127061. http://dx.doi.org/10.1016/j.amc.2022.127061.
[13] Preisser EL, Bolnick DI. The many faces of fear: comparing the pathways and impacts of nonconsumptive predator effects on prey populations. PLoS One 2008;3:e2465. http://dx.doi.org/10.1371/journal.pone.0002465.
[14] Tripathi JP, Bugalia S, Jana D, Gupta N, Tiwari V, Li J, Sun GQ. Modeling the cost of anti-predator strategy in a predator–prey system: The roles of indirect effect. Math Methods Appl Sci 2022;45:4365–96. http://dx.doi.org/10.1002/mma.8044.
[15] Zanette LY, White AF, Allen MC, Clinchy M. Perceived predation risk reduces the number of offspring songbirds produce per year. Science 2011;334:1398–401. http://dx.doi.org/10.1126/science.1210908.
[16] Nelson EH, Matthews CE, Rosenheim JA. Predators reduce prey population growth by inducing changes in prey behavior. Ecology 2004;85:1853–8. http://dx.doi.org/10.1890/03-3109.

[17] Preisser EL, Bolnick DI, Benard MF. Scared to death? The effects of intimidation and consumption in predator–prey interactions. Ecology 2005;86:501–9. http://dx.doi.org/10.1890/04-0719.

[18] Clinchy M, Sheriff MJ, Zanette LY. Predator-induced stress and the ecology of fear. Funct Ecol 2013;27:56–65. http://dx.doi.org/10.1111/1365-2435.12007.

[19] Hua F, Sieving KE, Fletcher Jr RJ, Wright CA. Increased perception of predation risk to adults and offspring alters avian reproductive strategy and performance. Behav Ecol 2014;25:509–19. http://dx.doi.org/10.1093/beheco/aru017.

[20] Cherry MJ, Morgan KE, Rutledge BT, Conner LM, Warren RJ. Can coyote predation risk induce reproduction suppression in white-tailed deer? Ecosphere 2016;7:e01481. http://dx.doi.org/10.1002/ecs2.1481.

[21] Tripathi Deepak, Singh Anuraj. An eco-epidemiological model with predator switching behavior. Comput Math Biophys 2023;11(1):20230101. http://dx.doi.org/10.1515/cmb-2023-0101.

[22] Li J, Sun GQ, Jin Z. Interactions of time delay and spatial diffusion induce the periodic oscillation of the vegetation system. Discrete Contin Dyn Syst B 2022;27:2147–72. http://dx.doi.org/10.3934/dcdsb.2021127.

[23] Møller AP, Christiansen SS, Mousseau TA. Sexual signals, risk of predation and escape behavior. Behav Ecol 2011;22:800–7. http://dx.doi.org/10.1093/beheco/arr046.

[24] Mpemba H, Karanja H, Jiang G. Predation fear, prey behavior, and community structure: a brief review of their relationship. Am Int J Biol 2019;7:1–7. http://dx.doi.org/10.15640/aijb.v7n1a1.

[25] Wang XY, Zanette L, Zou XF. Modelling the fear effect in predator–prey interactions. J Math Biol 2016;73:1179–204. http://dx.doi.org/10.1007/s00285-016-0989-1.

[26] Das A, Samanta GP. Modeling the fear effect on a stochastic prey–predator system with additional food for the predator. J Phys A 2018;51:465601. http://dx.doi.org/10.1088/1751-8121/aae4c6.

[27] Duan D, Niu B, Wei J. Hopf-Hopf bifurcation and chaotic attractors in a delayed diffusive predator–prey model with fear effect. Chaos Solitons Fractals 2019;123:206–16. http://dx.doi.org/10.1016/j.chaos.2019.04.012.

[28] Mondal S, Maiti A, Samanta GP. Effects of fear and additional food in a delayed predator–prey model. Biophys Rev Lett 2018;13:157–77. http://dx.doi.org/10.1142/S1793048018500091.

[29] Pal S, Majhi S, Mandal S, Pal N. Role of fear in a predator–prey model with Beddington–DeAngelis functional response. Z Natforsch A 2019;74:581–95. http://dx.doi.org/10.1515/zna-2018-0449.

[30] Pal S, Pal N, Samanta S, Chattopadhyay J. Fear effect in prey and hunting cooperation among predators in a Leslie–Gower model. Math Biosci Eng 2019;16:5146–79. http://dx.doi.org/10.3934/mbe.2019258.

[31] Roy J, Alam S. Fear factor in a prey–predator system in deterministic and stochastic environment. Phys A 2020;541:123359. http://dx.doi.org/10.1016/j.physa.2019.123359.

[32] Wang J, Cai Y, Fu S, Wang W. The effect of the fear factor on the dynamics of a predator–prey model incorporating the prey refuge. Chaos 2019;29:083109. http://dx.doi.org/10.1063/1.5111121.

[33] Wang XY, Zou XF. Modeling the fear effect in predator–prey interactions with adaptive avoidance of predators. Bull Math Biol 2017;79:1325–59. http://dx.doi.org/10.1007/s11538-017-0287-0.

[34] Zhang H, Cai Y, Fu S, Wang W. Impact of the fear effect in a prey-predator model incorporating a prey refuge. Appl Math Comput 2019;356:328–37. http://dx.doi.org/10.1016/j.amc.2019.03.034.

[35] Asamoah JKK, Safianu B, Afrifa E, Obeng B, Seidu B, Wireko FA, Sun GQ. Optimal control dynamics of Gonorrhea in a structured population. Heliyon 2023;9(10). http://dx.doi.org/10.1016/j.heliyon.2023.e20531.

[36] Seidu B, Asamoah JKK, Wiah EN, Ackora-Prah J. A comprehensive cost-effectiveness analysis of control of maize streak virus disease with Holling's Type II predation form and standard incidence. Results Phys 2022;40:105862. http://dx.doi.org/10.1016/j.rinp.2022.105862.

[37] Ackora-Prah J, Seidu B, Okyere E, Asamoah JKK. Fractal-fractional caputo maize streak virus disease model. Fractal Fract 2023;7(2):189. http://dx.doi.org/10.3390/fractalfract7020189.

[38] Seidu B, Makinde OD, Asamoah JKK. Threshold quantities and Lyapunov functions for ordinary differential equations epidemic models with mass action and standard incidence functions. Chaos Solitons Fractals 2023;170:113403. http://dx.doi.org/10.1016/j.chaos.2023.113403.

[39] Kar TK. Stability analysis of a prey–predator model incorporating a prey refuge. Commun Nonlinear Sci Numer Simul 2005;10:681–91. http://dx.doi.org/10.1016/j.cnsns.2003.08.006.

[40] Dawed MY, Koya PR, Mekonen TT. Generalist species predator–prey model and maximum sustainable yield. IOSR J Math 2016;12:13–24. http://dx.doi.org/10.9790/5728-1206051324.

[41] Sarwardi S, Mandal PK, Ray S. Dynamical behaviour of a two-predator model with prey refuge. J Biol Phys 2013;39:701–22. http://dx.doi.org/10.1007/s10867-013-9327-7.

[42] Sarwardi S, Mandal PK, Ray S. Analysis of a competitive prey–predator system with a prey refuge. Biosystems 2012;110:133–48. http://dx.doi.org/10.1016/j.biosystems.2012.08.002.

[43] Tripathi JP, Abbas S, Thakur M. A density dependent delayed predator–prey model with Beddington–DeAngelis type function response incorporating a prey refuge. Commun Nonlinear Sci Numer Simul 2015;22:427–50. http://dx.doi.org/10.1016/j.cnsns.2014.08.018.

[44] Singh Anuraj, Tripathi Deepak, Kang Yun. A modified May Holling Tanner model: The role of dynamic alternative resources on species' survival. J Biol Systems 2023. http://dx.doi.org/10.1142/S0218339024500074.

[45] Jana D, Agrawal R, Upadhyay RK. Dynamics of generalist predator in a stochastic environment: effect of delayed growth and prey refuge. Appl Math Comput 2015;268:1072–94. http://dx.doi.org/10.1016/j.amc.2015.06.098.

[46] Jana D, Tripathi JP. Impact of generalist type sexually reproductive top predator interference on the dynamics of a food chain model. Int J Dyn Control 2017;5:999–1009. http://dx.doi.org/10.1007/s40435-016-0255-9.

[47] Agrawal R, Jana D, Upadhyay RK, Rao VSH. Complex dynamics of sexually reproductive generalist predator and gestation delay in a food chain model: double Hopf-bifurcation to chaos. J Appl Math Comput 2017;55:513–47. http://dx.doi.org/10.1007/s12190-016-1048-1.

[48] Beddington JR. Mutual interference between parasites or predators and its effect on searching efficiency. J Anim Ecol 1975;44:331–40. http://dx.doi.org/10.2307/3866.

[49] DeAngelis DL, Goldstein RA, O'Neill RV. A model for tropic interaction. Ecology 1975;56:881–92. http://dx.doi.org/10.2307/1936298.

[50] Dubey B, Chandra P, Sinha P. A model for fishery resource with reserve area. Nonlinear Anal Real World Appl 2003;4:625–37. http://dx.doi.org/10.1016/S1468-1218(02)00082-2.

[51] Jana D. Chaotic dynamics of a discrete predator–prey system with prey refuge. Appl Math Comput 2013;224:848–65. http://dx.doi.org/10.1016/j.amc.2013.09.001.

[52] Ma ZH, Wang SF, Li WD, Li ZZ. The effect of prey refuge in a patchy predator–prey system. Math Biosci 2013;243:126–30. http://dx.doi.org/10.1016/j.mbs.2013.02.011.

[53] McNair JN. The effects of refuges on predator–prey interactions: a reconsideration. Theor Popul Biol 1986;29:38–63. http://dx.doi.org/10.1016/0040-5809(86)90004-3.

[54] Sun GQ, Zhang HT, Song YL, Li L, Jin Z. Dynamic analysis of a plant-water model with spatial diffusion. J Differential Equations 2022;329:395–430. http://dx.doi.org/10.1016/j.jde.2022.05.009.

[55] González-Olivares E, Ramos-Jiliberto R. Dynamic consequences of prey refuges in a simple model system: more prey, fewer predators and enhanced stability. Ecol Model 2003;166:135–46. http://dx.doi.org/10.1016/S0304-3800(03)00131-5.

[56] Tripathi JP. Almost periodic solution and global attractivity for a density dependent predator–prey system with mutual interference and Crowley–Martin response function. Differ Equ Dyn Syst 2020;28:19–37. http://dx.doi.org/10.1007/s12591-016-0298-6.

[57] Tripathi JP, Abbas S, Thakur M. Dynamical analysis of a prey–predator model with Beddington–DeAngelis type function response incorporating a prey refuge. Nonlinear Dynam 2015;80:177–96. http://dx.doi.org/10.1007/s11071-014-1859-2.

[58] Guan XN, Wang WM, Cai YL. Spatiotemporal dynamics of a Leslie–Gower predator–prey model incorporating a prey refuge. Nonlinear Anal Real World Appl 2011;12:2385–95. http://dx.doi.org/10.1016/j.nonrwa.2011.02.011.

[59] Jana S, Chakraborty M, Chakraborty K, Kar TK. Global stability and bifurcation of time delayed prey–predator system incorporating prey refuge. Math Comput Simulation 2012;85:57–77. http://dx.doi.org/10.1016/j.matcom.2012.10.003.

[60] Ko W, Ryu K. Qualitative analysis of a predator–prey model with Holling type II functional response incorporating a prey refuge. J Differential Equations 2006;231:534–50. http://dx.doi.org/10.1016/j.jde.2006.08.001.

[61] Lian X, Wang H, Wang W. Delay-driven pattern formation in a reaction–diffusion predator–prey model incorporating a prey refuge. J Stat Mech Theory Exp 2013;P04006. http://dx.doi.org/10.1088/1742-5468/2013/04/P04006.

[62] Lian X, Yan SL, Wang HL. Pattern formation in predator–prey model with delay and cross diffusion. Abstr Appl Anal 2013;147232. http://dx.doi.org/10.1155/2013/147232.

[63] Magalhaes S, van Rijn PCJ, Montserrat M, Pallini A, Sabelis MW. Population dynamics of thrips prey and their mite predators in a refuge. Oecologia 2007;150:557–68. http://dx.doi.org/10.1007/s00442-006-0548-3.

[64] Souna F, Lakmeche A, Djilali S. Spatiotemporal patterns in a diffusive predator–prey model with protection zone and predator harvesting. Chaos Solitons Fractals 2020;140:110180. http://dx.doi.org/10.1016/j.chaos.2020.110180.

[65] Tripathi JP, Jana D, Vyshnavi Devi NSNVK, Tiwari V, Abbas S. Intraspecific competition of predator for prey with variable rates in protected areas. Nonlinear Dynam 2020;102:511–35. http://dx.doi.org/10.1007/s11071-020-05951-6.

[66] Cantrell RS, Cosner C. Spatial ecology via reaction–diffusion equations. John Wiley & Sons; 2004.

[67] Neuhauser C. Mathematical challenges in spatial ecology. Notices Amer Math Soc 2001;48:1304–14.
[68] Alkhamis MA, Youha SA, Khajah MM, Haider NB, Alhardan S, Nabeel A, Mazeedi SA, Al-Sabah SK. Spatiotemporal dynamics of the COVID-19 pandemic in the State of Kuwait. Int J Infect Dis 2020;98:153–60. http://dx.doi.org/10.1016/j.ijid.2020.06.078.
[69] Andersen H, Cermak J, Solodovnik I, Lelli L, Vogt R. Spatiotemporal dynamics of fog and low clouds in the Namib unveiled with ground-and space-based observations. Atmos Chem Phys 2019;19:4383–92. http://dx.doi.org/10.5194/acp-19-4383-2019.
[70] Bießmann F, Papaioannou J-M, Harth A, Jugel ML, Müller K-R, Braun M. Quantifying spatiotemporal dynamics of twitter replies to news feeds. In: 2012 IEEE international workshop on machine learning for signal processing. IEEE; 2012, p. 1–6.
[71] D'Souza AW, Potter RF, Wallace M, Shupe A, Patel S, Sun XQ, Gul D, et al. Spatiotemporal dynamics of multidrug resistant bacteria on intensive care unit surfaces. Nature Commun 2019;10:1–19. http://dx.doi.org/10.1038/s41467-019-12563-1.
[72] Fuchs S, Keiler M, Sokratov S, Shnyparkov A. Spatiotemporal dynamics: the need for an innovative approach in mountain hazard risk management. Nat Hazards 2013;68:1217–41. http://dx.doi.org/10.1007/s11069-012-0508-7.
[73] Liao C, Clark PE, Shibia M, DeGloria SD. Spatiotemporal dynamics of cattle behavior and resource selection patterns on East African rangelands: evidence from GPS-tracking. Int J Geogr Inf Sci 2018;32:1523–40. http://dx.doi.org/10.1080/13658816.2018.1424856.
[74] Marinković K. Spatiotemporal dynamics of word processing in the human cortex. Neuroscientist 2004;10:142–52. http://dx.doi.org/10.1177/1073858403261018.
[75] Li J, Sun GQ, Guo ZG. Bifurcation analysis of an extended Klausmeier–Gray–Scott model with infiltration delay. Stud Appl Math 2022;148:1519–42. http://dx.doi.org/10.1111/sapm.12482.
[76] Upadhyay RK, Wang WM, Thakur NK. Spatiotemporal dynamics in a spatial plankton system. Math Model Nat Phenom 2010;5:102–22. http://dx.doi.org/10.1051/mmnp/20105507.
[77] Wang GM. Spatiotemporal dynamics of mesocarnivore populations. Wildl Biol 2018;2018. http://dx.doi.org/10.2981/wlb.00429.
[78] Zhang J, Beusen AHW, Apeldoorn DFV, Mogollón JM, Yu C, Bouwman AF. Spatiotemporal dynamics of soil phosphorus and crop uptake in global cropland during the 20th century. Biogeosciences 2017;14:2055–68. http://dx.doi.org/10.5194/bg-14-2055-2017, 2017.
[79] Dai BX, Sun GX. Turing–Hopf bifurcation of a delayed diffusive predator–prey system with chemotaxis and fear effect. Appl Math Lett 2021;111:106644. http://dx.doi.org/10.1016/j.aml.2020.106644.
[80] Han R, Guin LN, Dai BX. Cross-diffusion-driven pattern formation and selection in a modified Leslie–Gower predator–prey model with fear effect. J Biol Syst 2020;28:27–64. http://dx.doi.org/10.1142/S0218339020500023.
[81] Shi Y, Wu JH, Cao Q. Analysis on a diffusive multiple Allee effects predator–prey model induced by fear factors. Nonlinear Anal Real World Appl 2021;59:103249. http://dx.doi.org/10.1016/j.nonrwa.2020.103249.
[82] Guin LN, Pal S, Chakravarty S, Djilali S. Pattern dynamics of a reaction–diffusion predator–prey system with both refuge and harvesting. Int J Biomath 2021;14:2050084. http://dx.doi.org/10.1142/S1793524520500849.
[83] Clinchy Michael, Sheriff Michael J, Zanette Liana Y. Predator-induced stress and the ecology of fear. Funct Ecol 2013;27(1):56–65. http://dx.doi.org/10.1111/1365-2435.12007.
[84] Leslie PH, Gower JC. The properties of a stochastic model for the predator–prey type of interaction between two species. Biometrika 1960;47(3/4):219–34. http://dx.doi.org/10.2307/2333294.
[85] Perko L. Nonlinear systems: Local theory. In: Differential equations and dynamical systems. New York, NY: Springer; 2001, p. 65–180.
[86] Dubey B, Hussain J. Modelling the interaction of two biological species in a polluted environment. J Math Anal Appl 2000;246(1):58–79. http://dx.doi.org/10.1006/jmaa.2000.6741.
[87] Sih A. Prey refuges and predator–prey stability. Theor Popul Biol 1987;31:1–12. http://dx.doi.org/10.1016/0040-5809(87)90019-0.
[88] Souna F, Djilali S, Lakmeche A. Spatiotemporal behavior in a predator–prey model with herd behavior and cross-diffusion and fear effect. Eur Phys J Plus 2021;136:1–21. http://dx.doi.org/10.1140/epjp/s13360-021-01489-7.